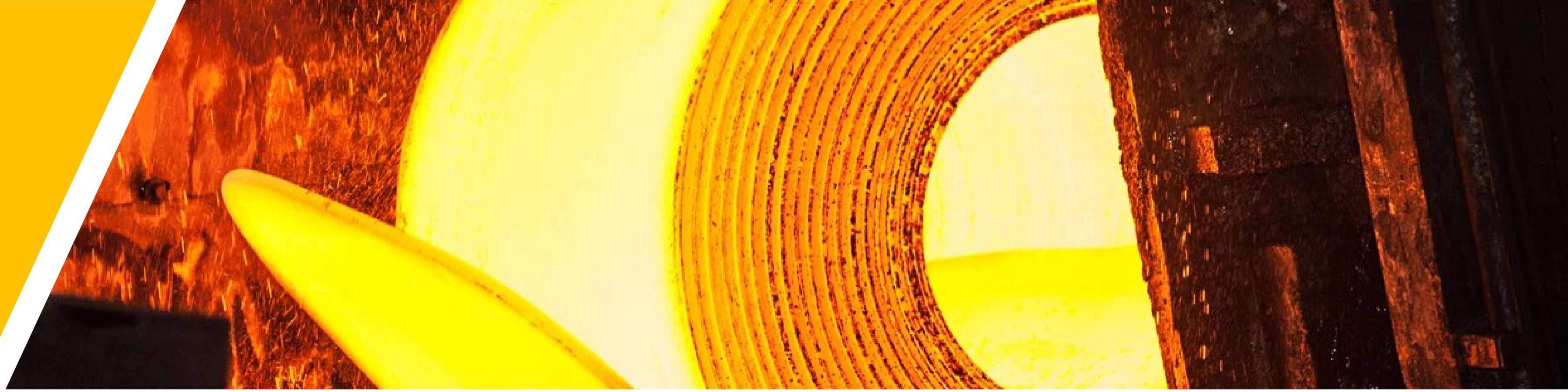

Intensive Recrystallization-Controlled Rolling of High-Temperature-Processing Linepipe Steel with Low Nb Content

Prof. C. Isaac Garcia

Ferrous Physical Metallurgy Group

University of Pittsburgh

Ferrous Physical Metallurgy Group

Tenaris

NUCOR

NUCOR BERKELEY

NUCOR DECATUR

Nucor Steel Arkansas

North Star BlueScope

Ternium

Hylsa
Siderar
Sidor

Mexico
Argentine

PA pennsylvania
DEPARTMENT OF COMMUNITY & ECONOMIC DEVELOPMENT

GKN SINTER METALS

UNIVERSAL STAINLESS
20 Years Serving Our Customers

USS

CLIFFS
CLEVELAND-CLIFFS INC.

CLIFFS
Riverdale

ArcelorMittal

ECG

ESS ELLWOOD SPECIALTY STEEL

Forging Foundation (FIERF)

FIERF
FORGING FOUNDATION

BRS
BIG RIVER STEEL
a U. S. Steel company

WHEMCO
Group of Companies

WORTHINGTON INDUSTRIES

EXAMPLES OF AREAS OF RESEARCH INTEREST TO THE FERROUS PHYSICAL METALLURGY GROUP

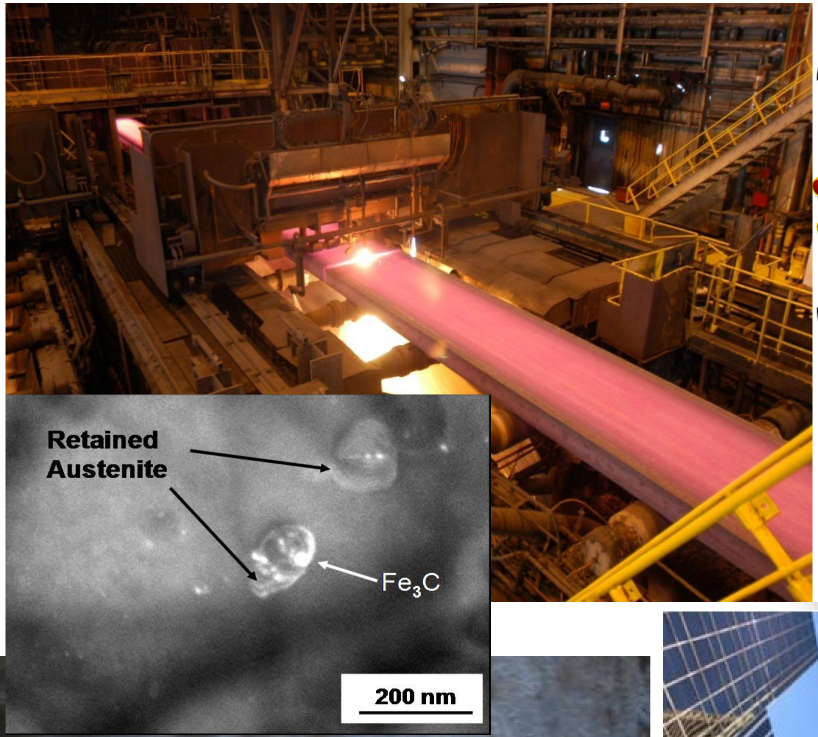

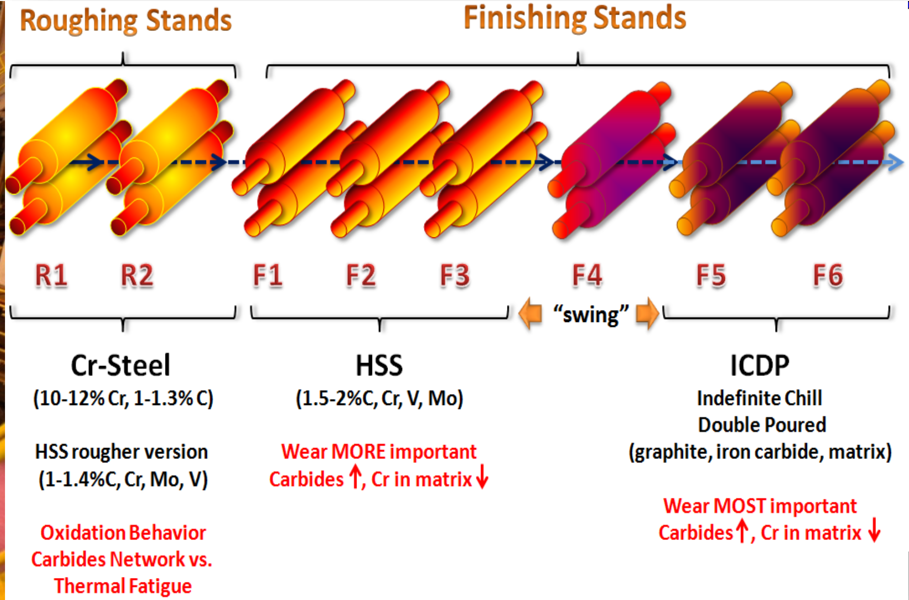

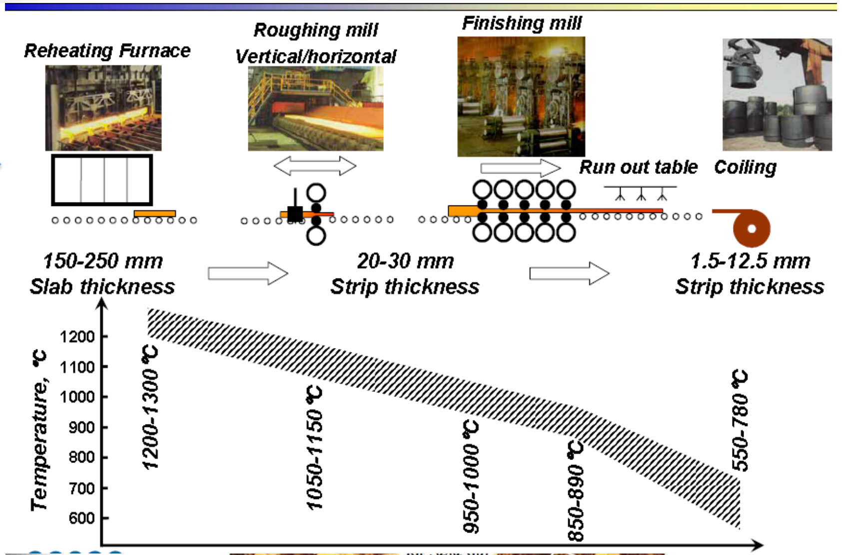

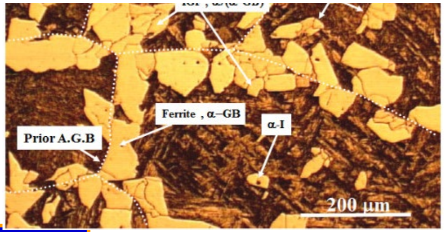

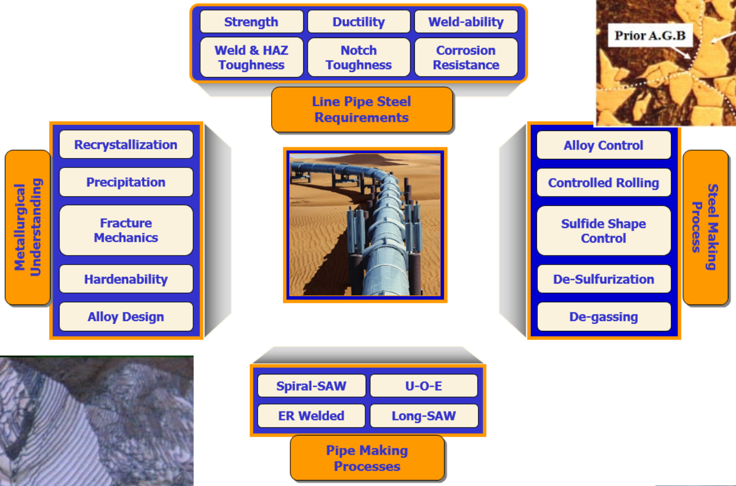

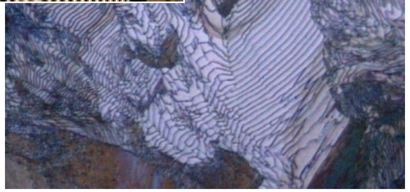

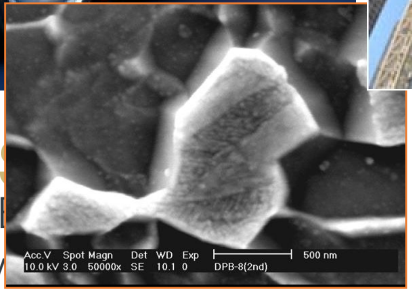

PITT

MECHANICAL & M

GOAL: *To develop a robust processing route to the production of High-Strength Low-Alloy (HSLA) steel for linepipe applications.*

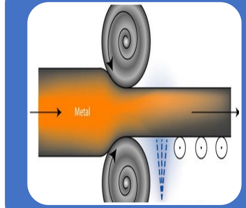

1.Intensive Recrystallization-Controlled Rolling + Accelerated Cooling.

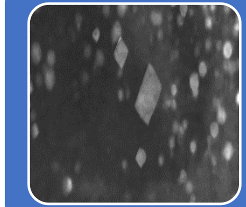

Optimize microstructure for properties.

Improve cost and productivity.

Hypothesis:

The precipitation and grain refinement required for the strength and toughness of a linepipe steel can be achieved by a novel hot deformation approach. This approach consists of increasing deformation at recrystallization conditions and using lower amounts of micro-alloying additions.

General Objective

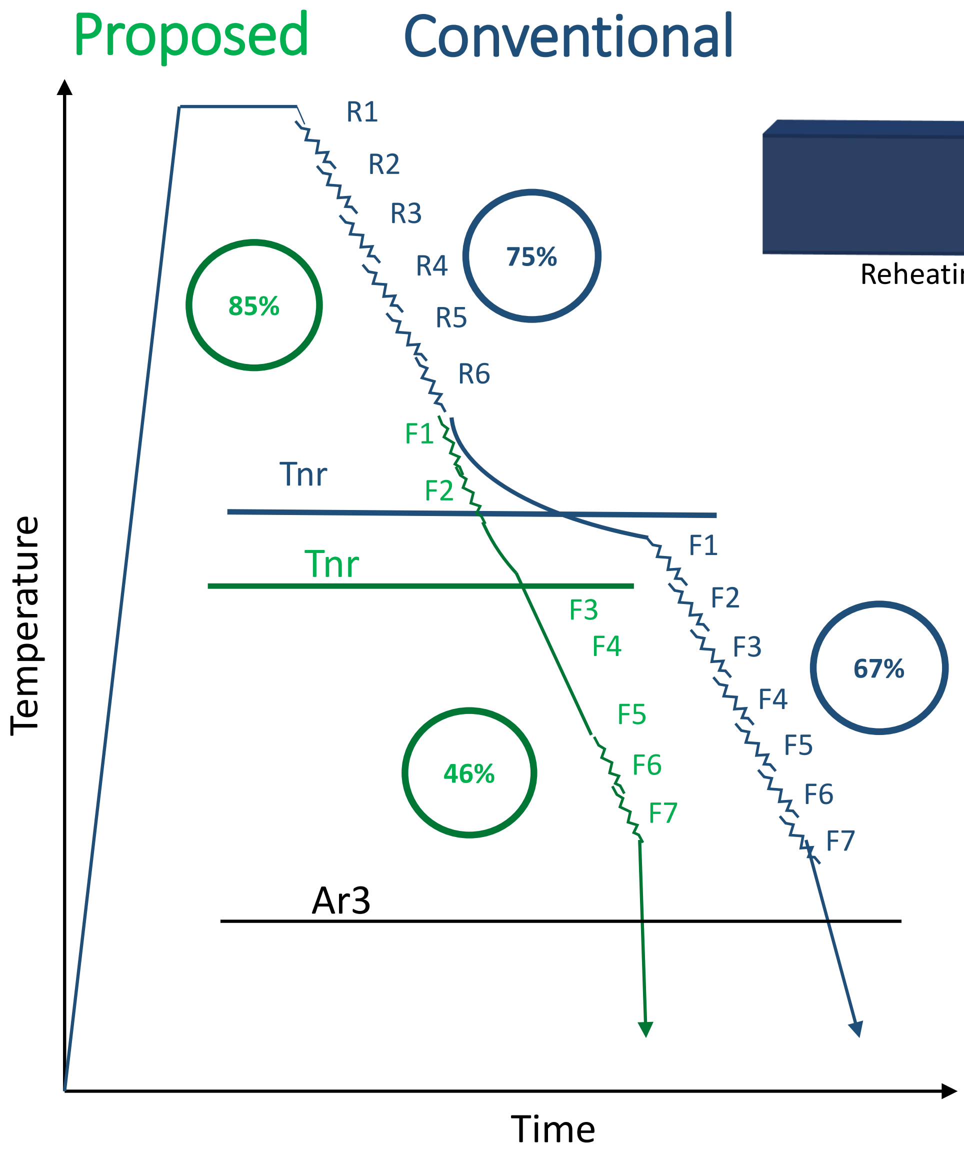

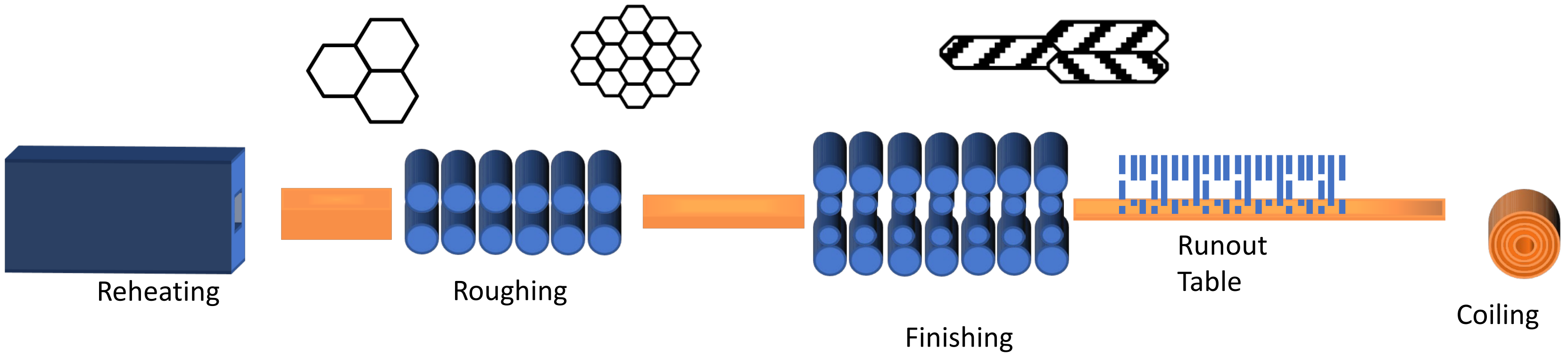

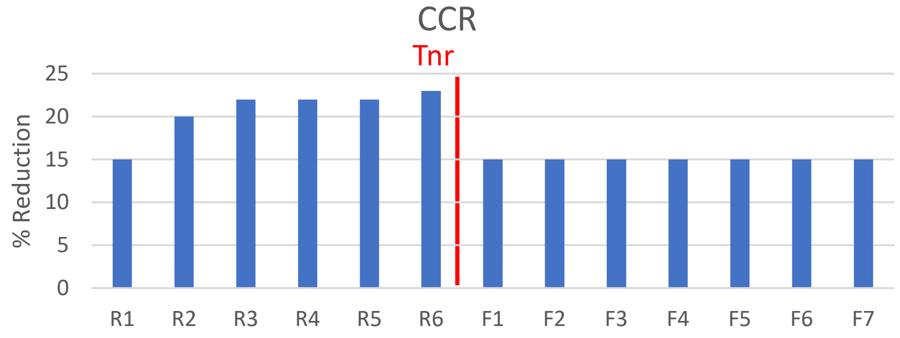

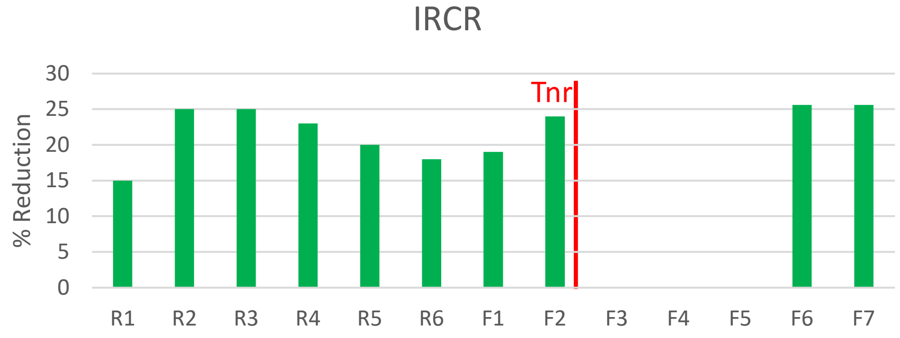

Overall Experimental Approach

Reheating Studies
- Grain coarsening
- Dissolution study

Hot Behavior
- MFS
- Recrystallization
- Precipitation studies

Hot Deformation and Transformation Simulations
- Austenite conditioning
- Ferrite formation
- Precipitation

Validation
- Full scale validation at experimental mill

Chemistries and Critical Temperatures

Wt%	Low Nb	Med Nb	High Nb
C	**0.050**	**0.049**	**0.049**
Mn	1.495	1.518	1.508
P	0.012	0.011	0.011
S	0.0044	0.0040	0.0045
Si	0.261	0.262	0.249
Cu	0.096	0.098	0.097
Ni	0.257	0.255	0.255
Cr	0.253	0.253	0.252
Mo	0.151	0.151	0.151
V	0.061	0.064	0.064
Ti	0.010	0.010	0.010
Al	0.032	0.034	0.035
N	0.0072	0.0065	0.0068
Nb	**0.051**	0.070	**0.091**
B	0.00	0.00	0.00
Ca	0.0012	0.0013	0.0015

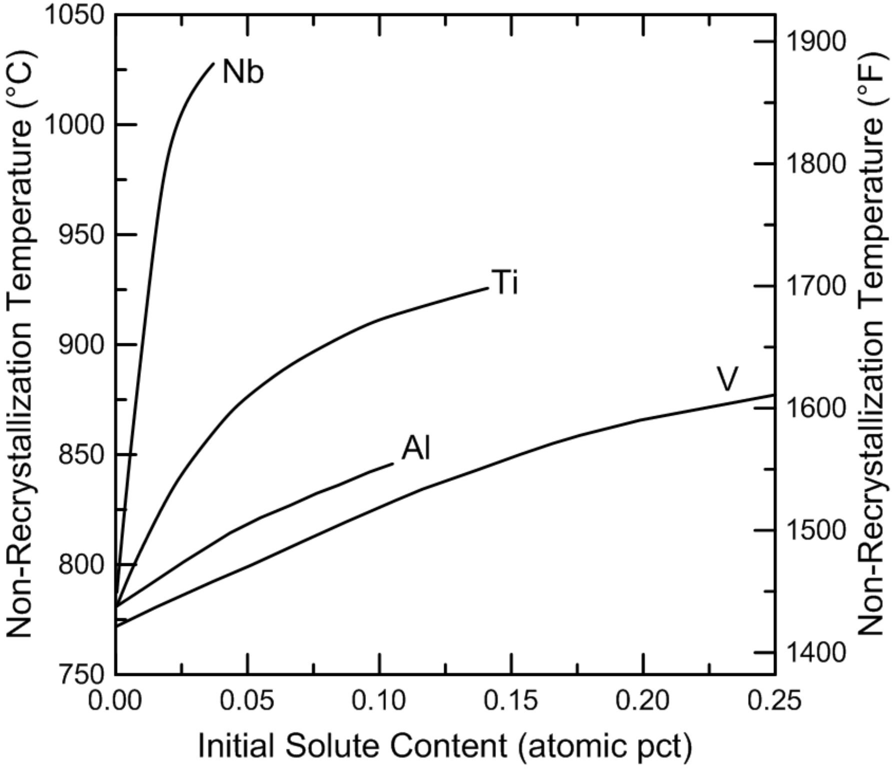

Palmiere 1996 Hutchinson 2008
Maruyama 1998 Jiao 2010
Siciliano 2000 Zhu 2015
Stahlheim 2005 Zhao 2016

	A_{r3}	A_{r1}
High-Nb	848°C	688°C
Low-Nb	847°C	689°C

1 2 3 4

Dissolution Predictions

$$[M]^m[N]^n = K \qquad K = K_o exp\frac{-\Delta H}{RT} \qquad K = logA - \frac{B}{T}$$

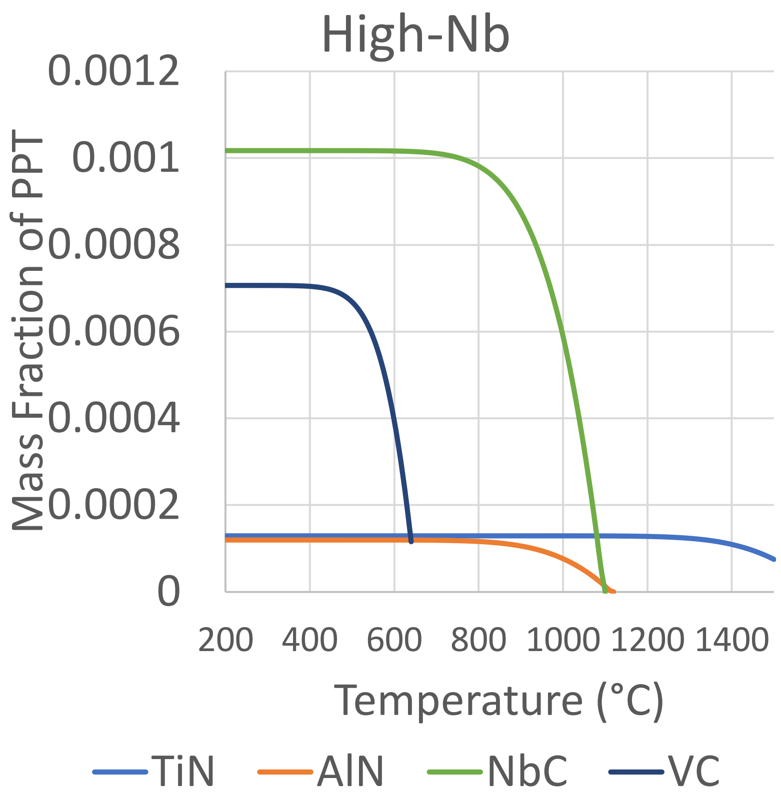

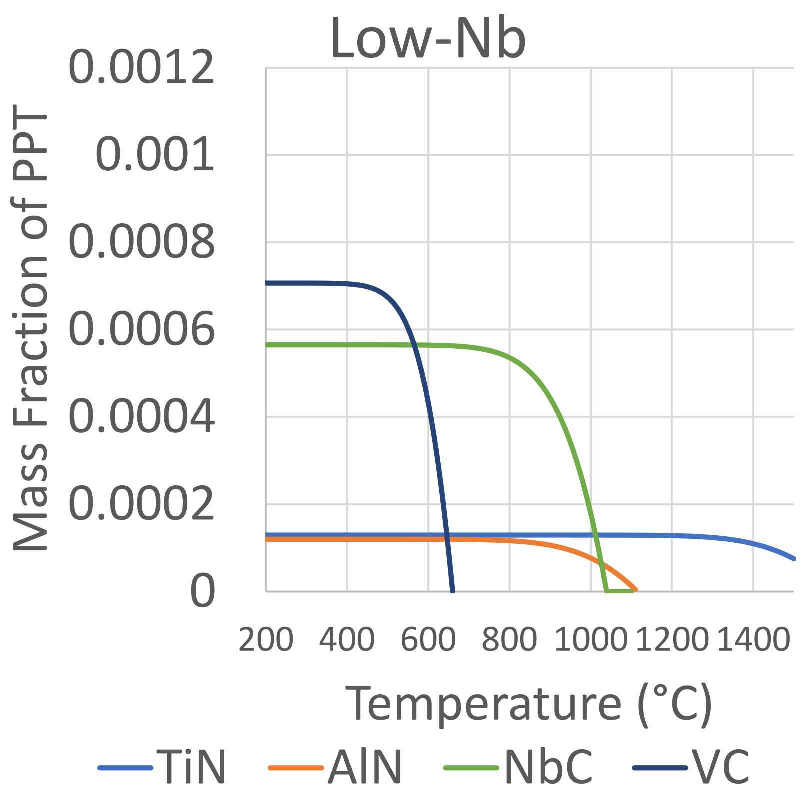

1 2 3 4

Austenite Grain Size Control with Low-Nb

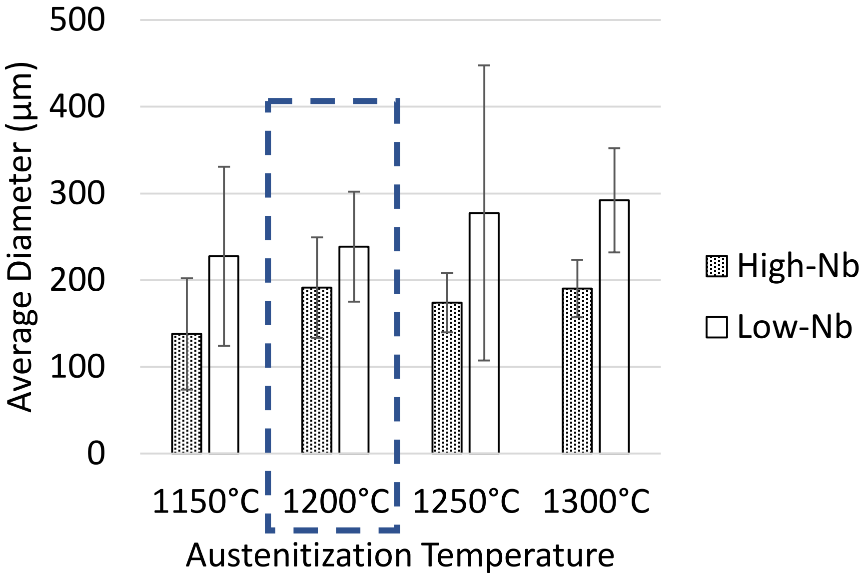

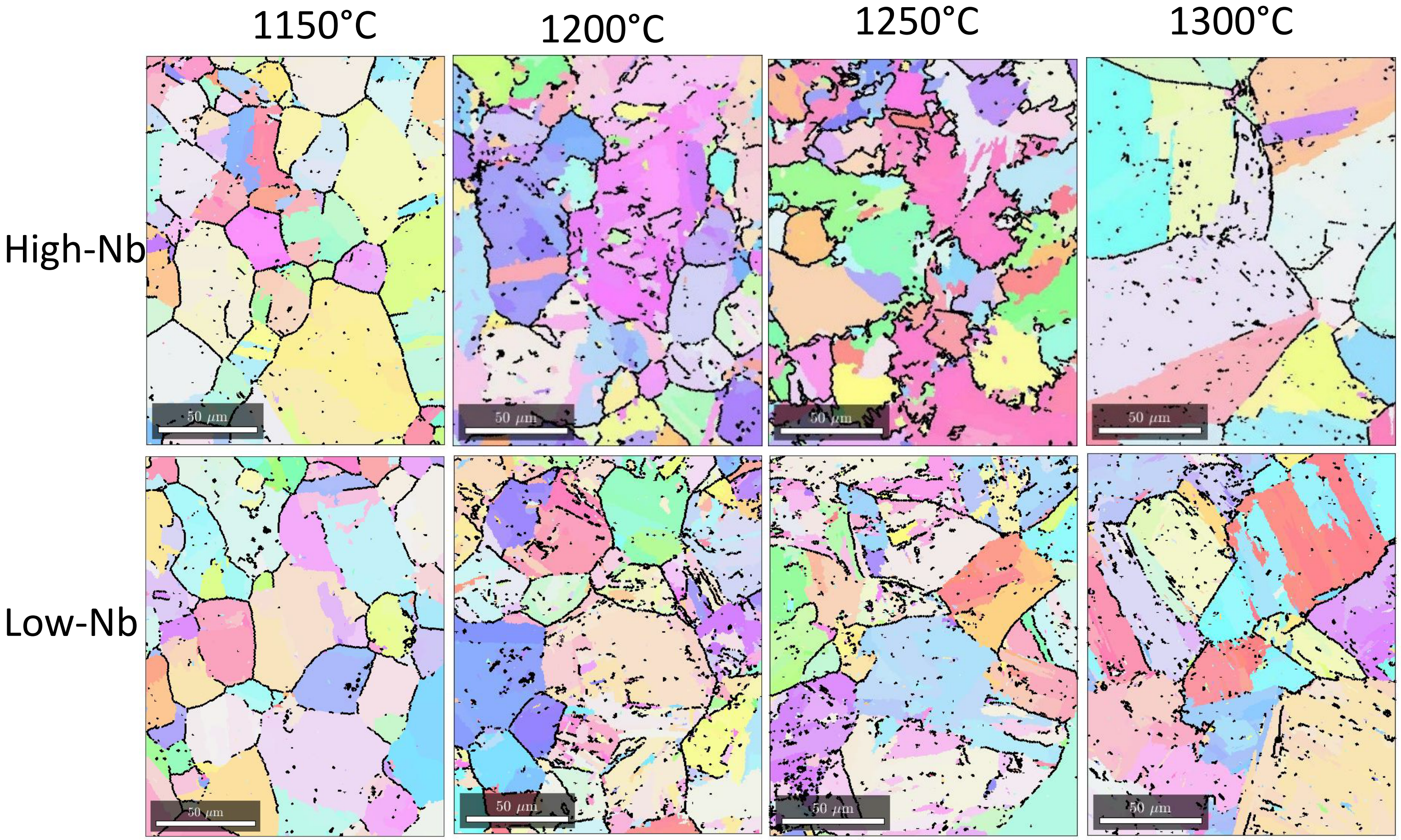

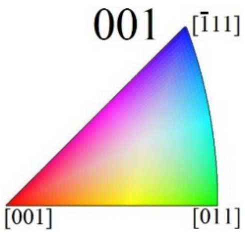

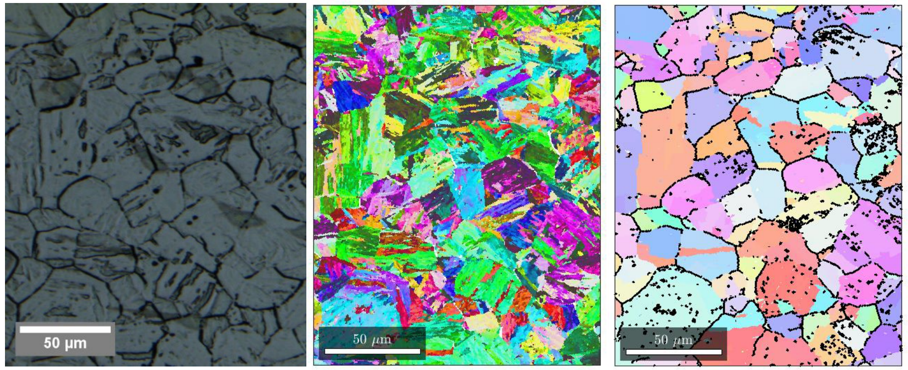

Nyyssönen, T., *et al* (2016)

Precipitation Dissolution Retarded by Particle Complexity

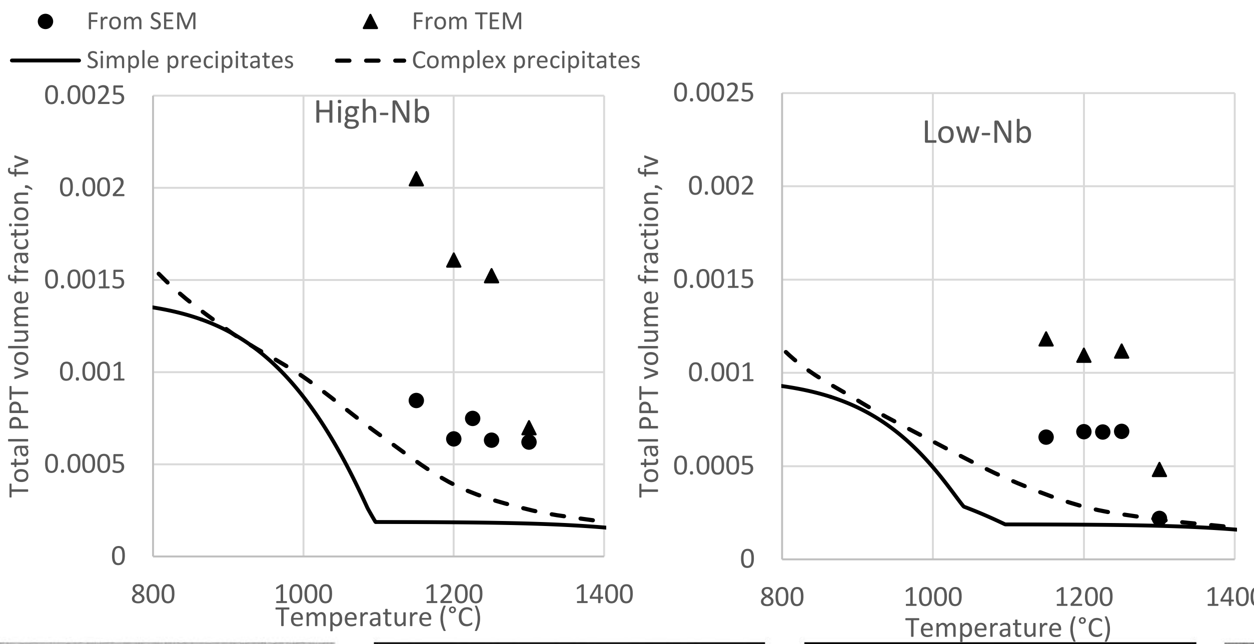

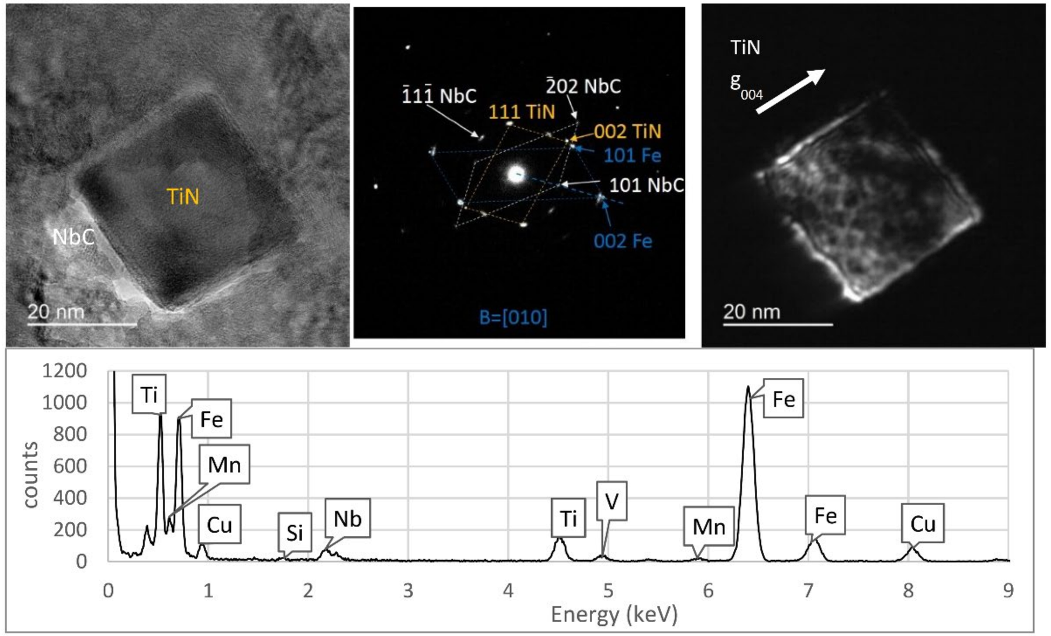

EDS	Si	Ti	V	Mn	Fe	Cu	Nb
At%/Wt%	0.94/0.5	10.09/8.6	0.69/0.6	1.08/1.1	78.07/77.5	6.37/7.2	2.77/4.6

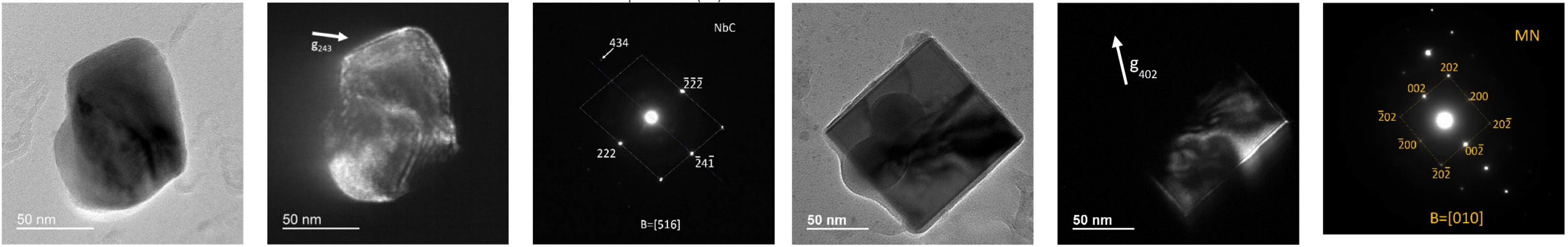

Similar Dissolution Behavior for Both Nb Contents

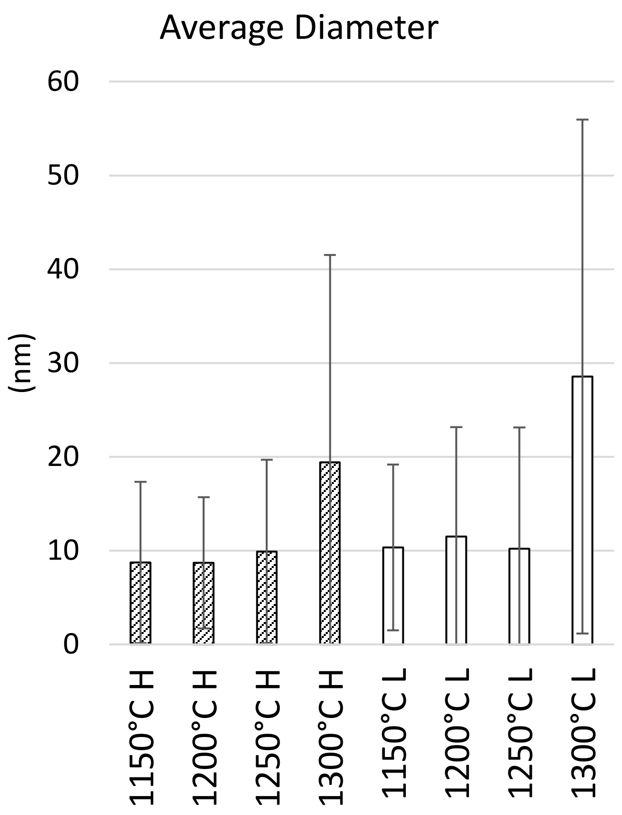

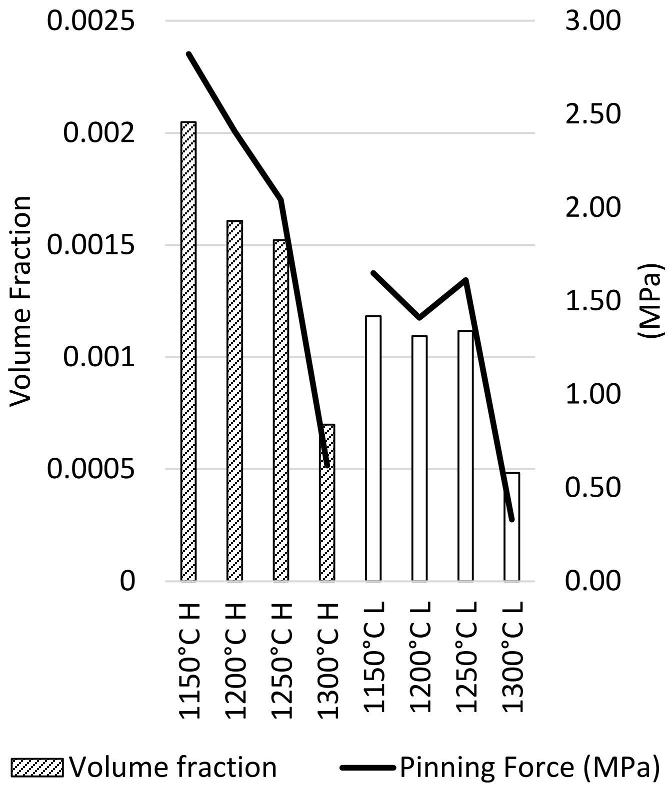

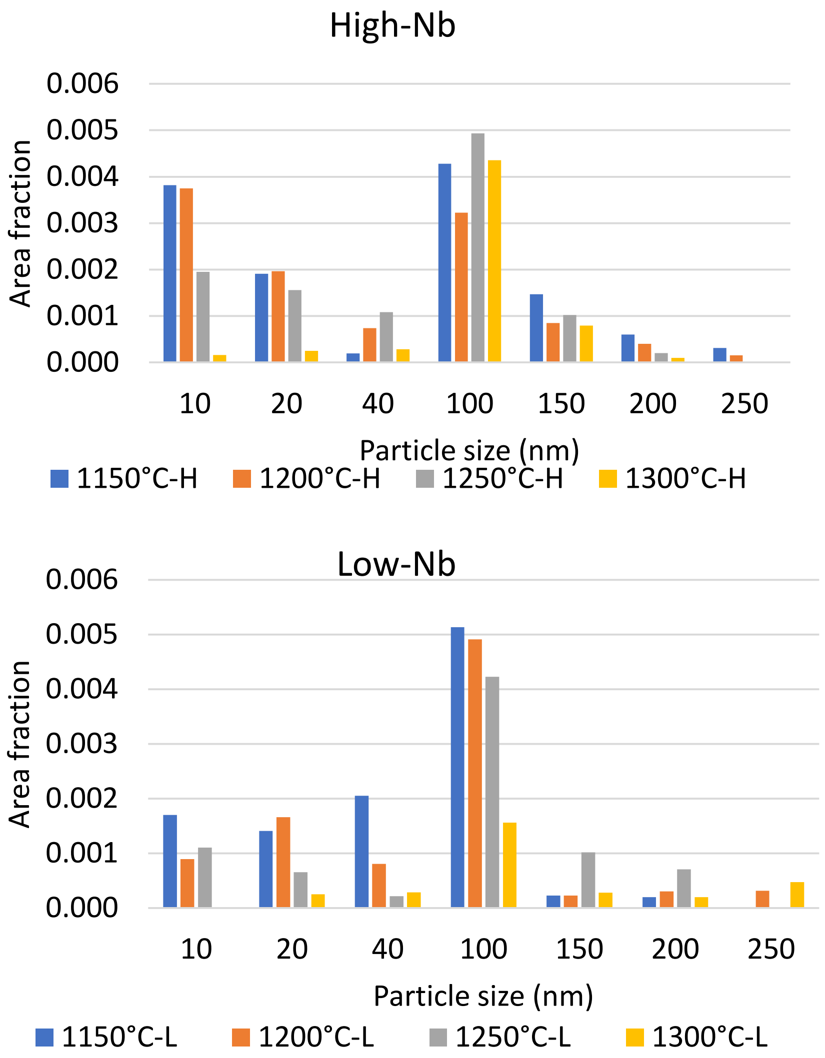

1 2 3 4

Reheating Summary

- PAGS:
  - Low-Nb steel maintains grain size control below 1200°C for 1h.
  - PAGS can be measured with EBSD reconstruction tools.
- Dissolution:
  - Experimental PPT volume fraction exceeded model predictions.
  - Remaining PPTs appear of complex composition and morphology. Ti-rich precipitates 100-300nm in size. Nb-rich PPTs 20-60nm in size.
  - Precipitates nature, morphology and size was verified by SEM, EDS, SADP and HRTEM.
  - There is an opportunity to model the kinetics of dissolution of complex particles

Experimental Approach - Results

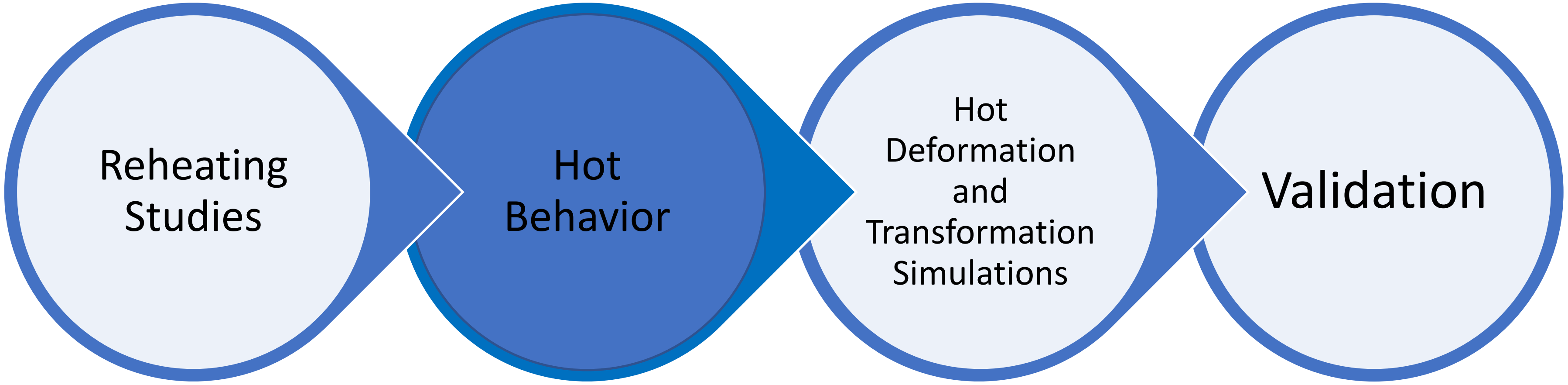

- Grain coarsening
- Dissolution study

- MFS
- Recrystallization
- Precipitation studies

- Austenite conditioning
- Ferrite formation
- Precipitation

- Full scale validation at experimental mill

University of Pittsburgh

Mean Flow Stress Matched Existing Models

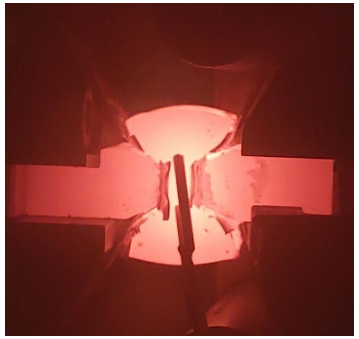

Misaka, Y., and T. Yoshimoto (1967)

$$MFS = e^{\left(0.126-1.75[C]+0.594[C]^2+\frac{2851+2968[C]-1120[C]^2}{T}\right)}\varepsilon^{0.21}\dot{\varepsilon}^{0.13}$$

Siciliano, *et al.* (1996)

$$MFS = (0.78 + 0.137[Mn]) * (MFS_{Misaka}) * (1 - X_{dyn}) + K\sigma_{ss}X_{dyn}$$

Experimental

$$MFS = \frac{1}{\varepsilon_1 - \varepsilon_0}\int_{\varepsilon_0}^{\varepsilon_1} \sigma \, d\varepsilon$$

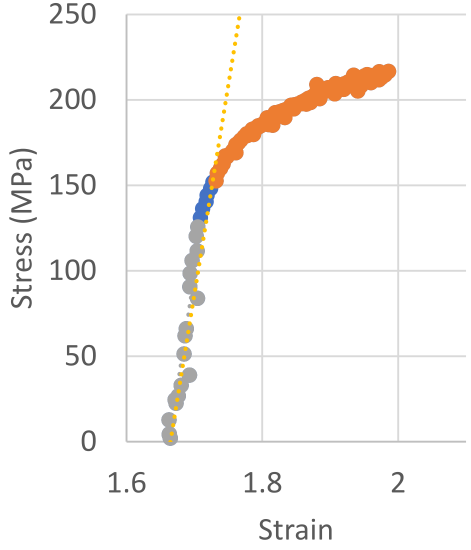

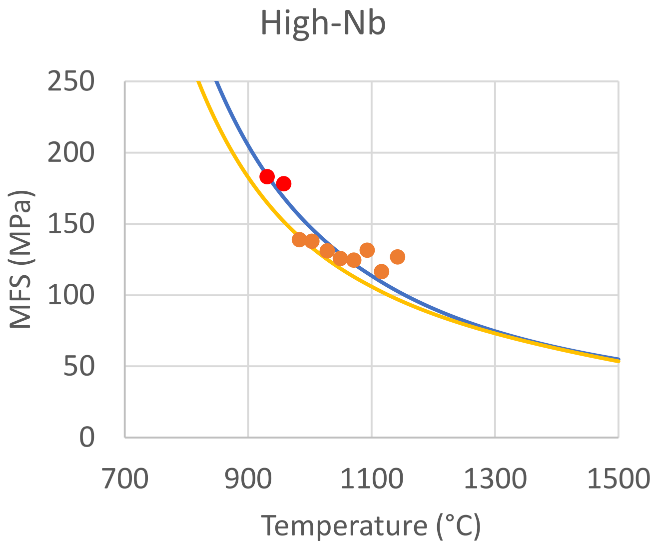

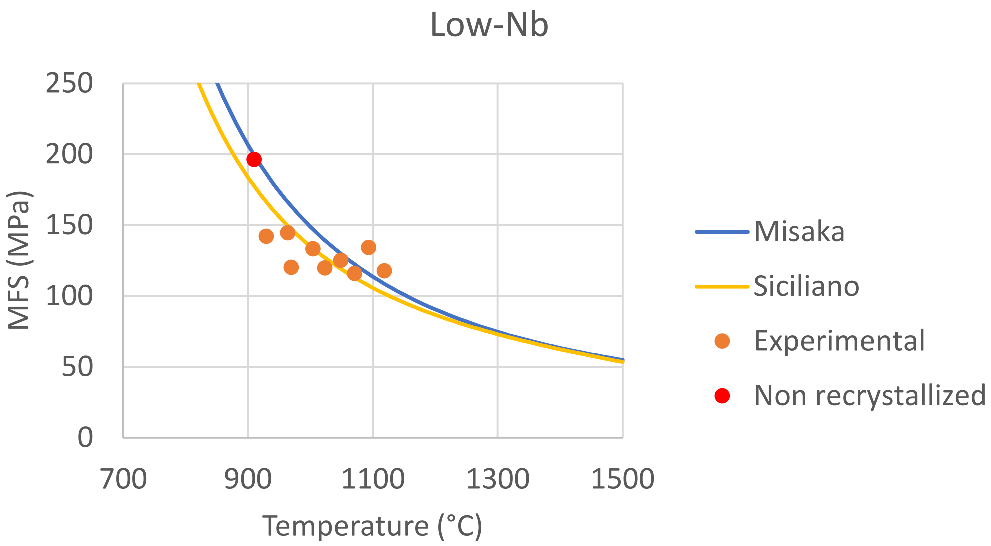

Hot Compression Experiments

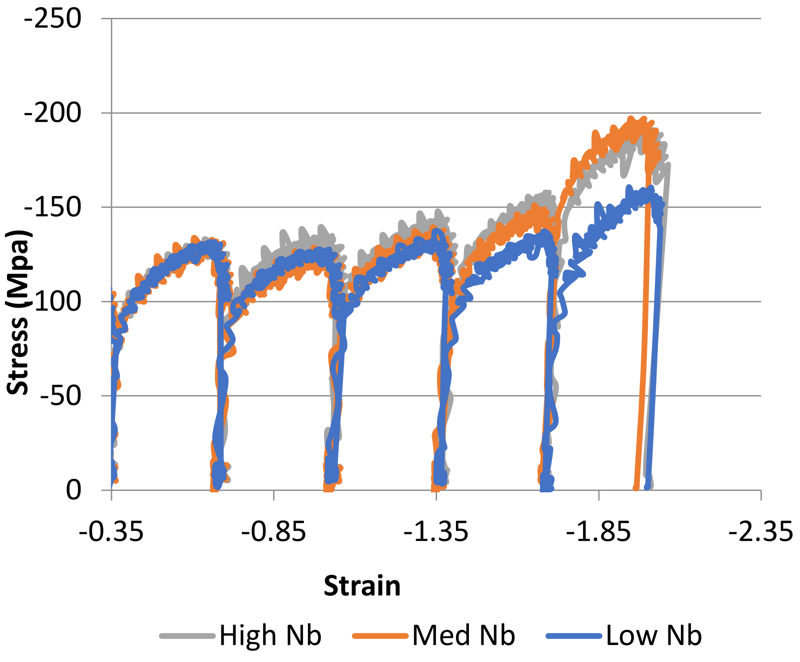

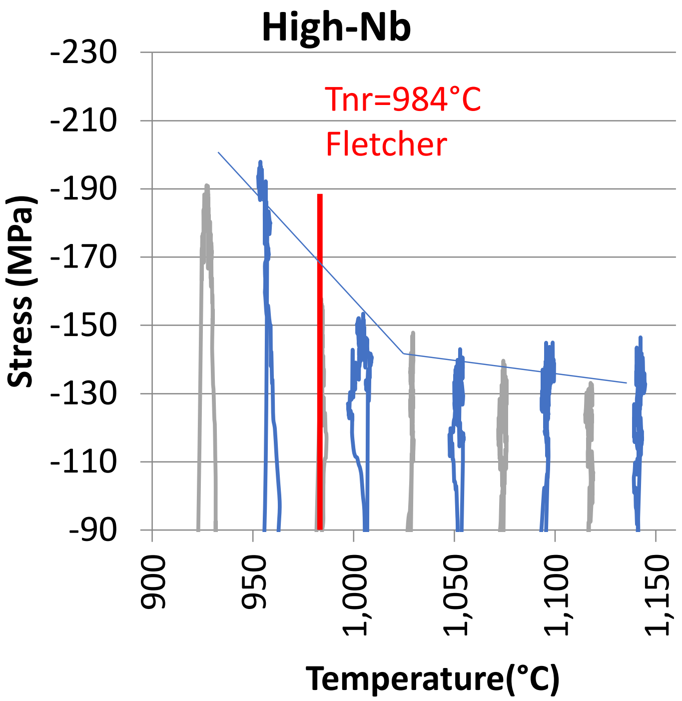

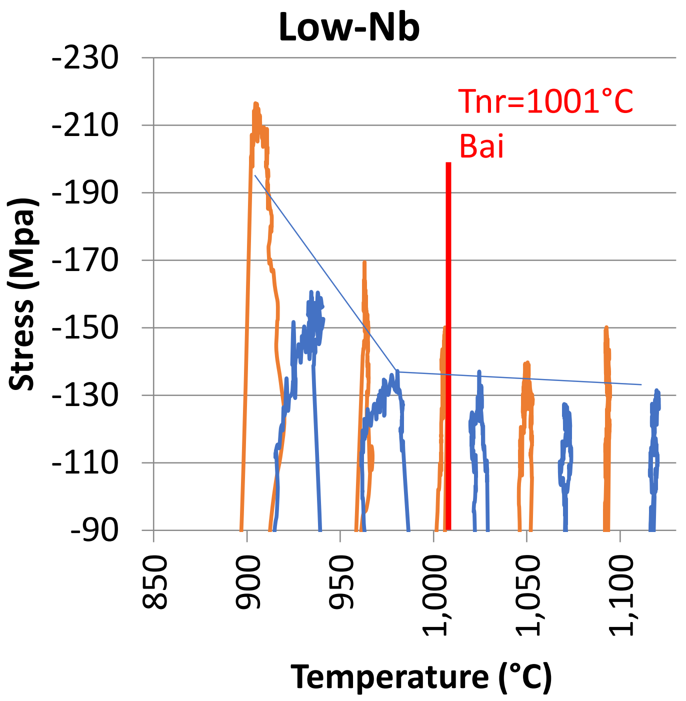

	Experimental Tnr	Boratto 1988	Fletcher 2008	Bai 2011
Low Nb	~975°C	1100°C	935°C	1001°C
High Nb	~1025°C	1309°C	984°C	1043°C

$$T_{NR} = 887 + 464C + \left(6445Nb - 644\sqrt{Nb}\right) + \left(732V - 230\sqrt{V}\right) + 890Ti + 363Al - 357Si$$

$$T_{NR} = 203 - 310C - 149\sqrt{V} + 657\sqrt{Nb} + 683e^{-0.36\varepsilon}$$

$$T_{NR} = 174\log\left[Nb\left(C + \frac{12}{14}N\right)\right] + 1444$$

1 2 3 4

What Controls Recrystallization Inhibition?

University of Pittsburgh

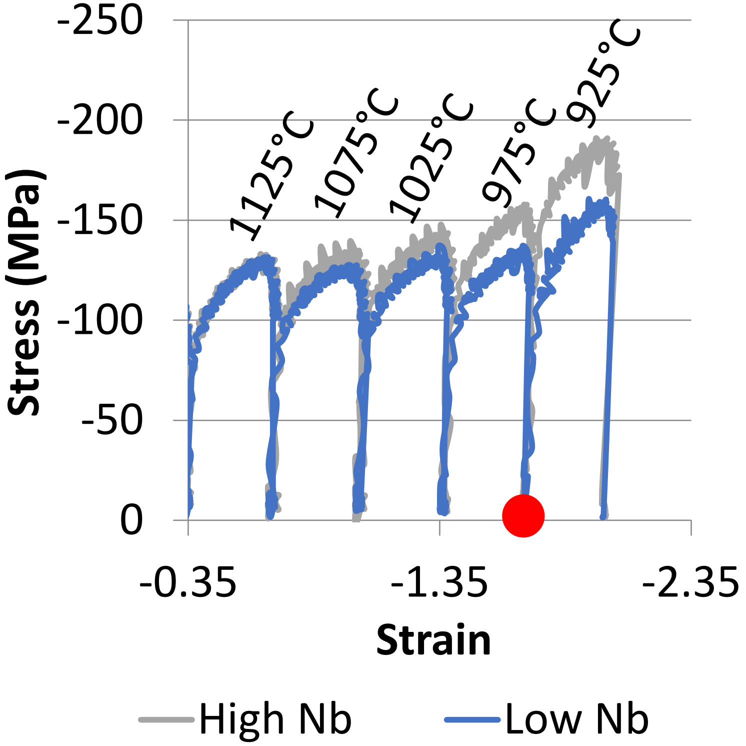

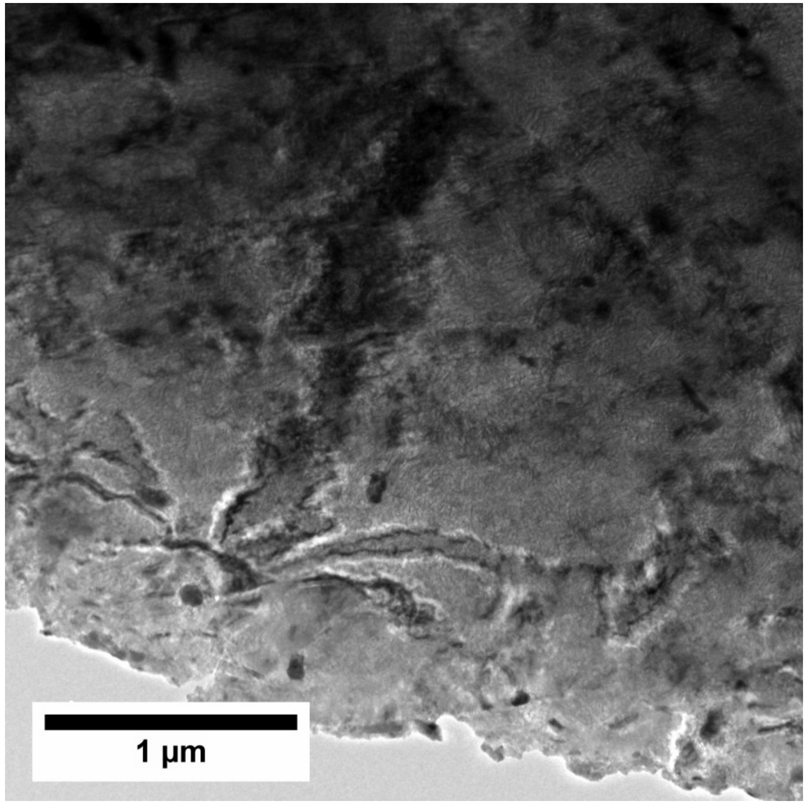

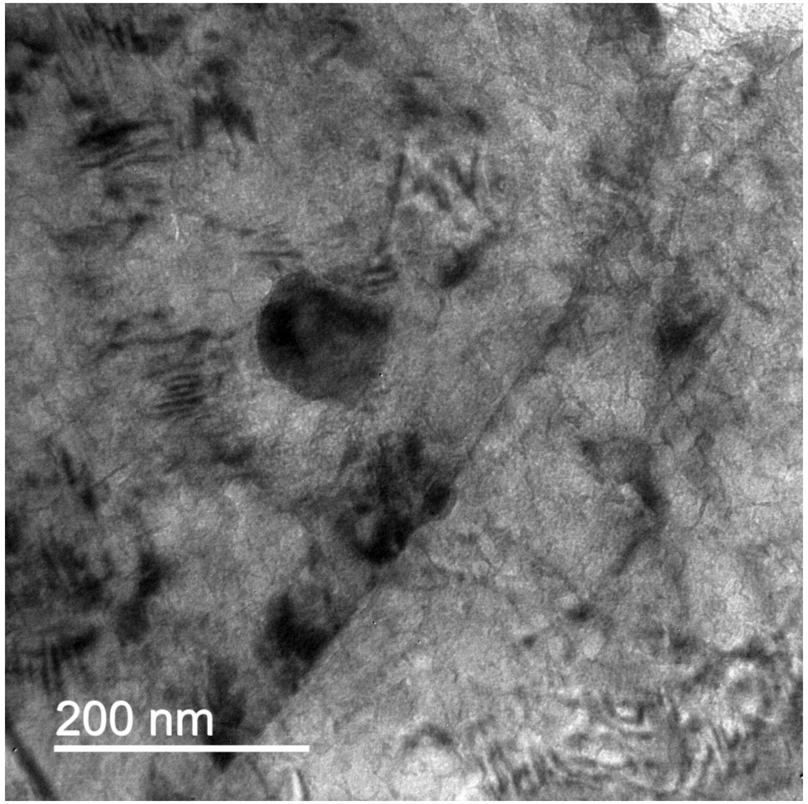

1 2 3 4

Precipitation prevents recrystallization

$F_{PIN} = 4r\sigma N_s$

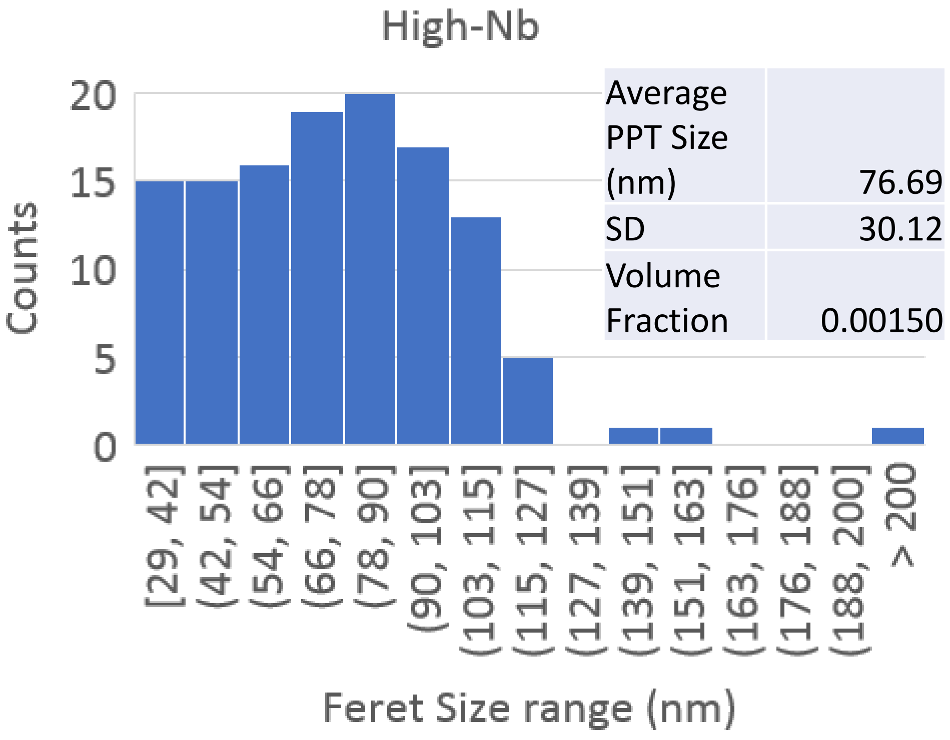

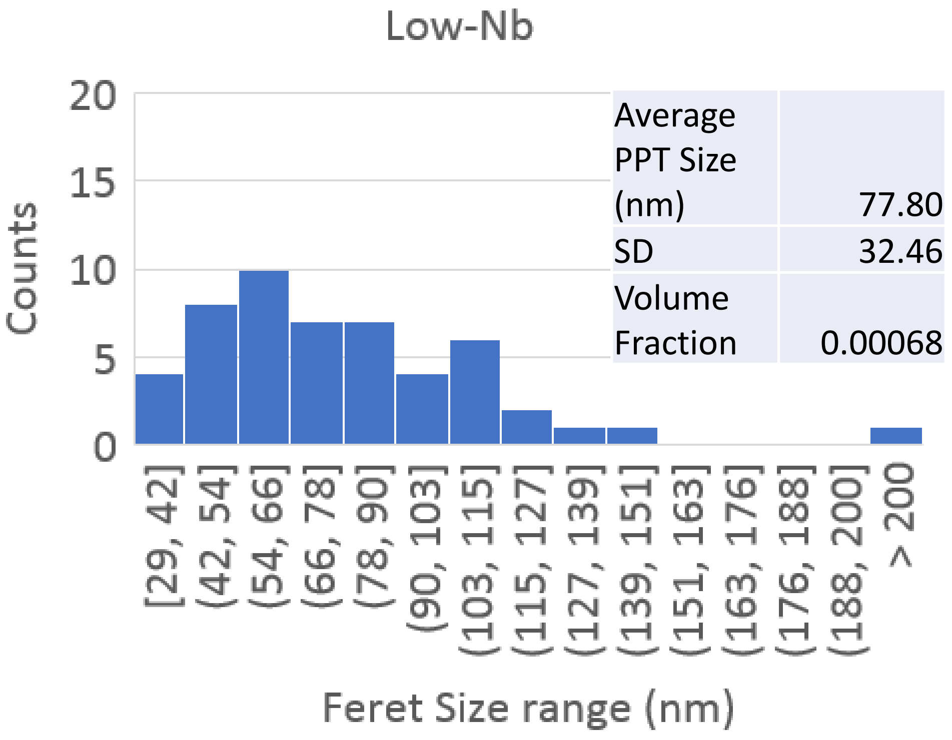

Zener: $F_{PIN} = 4r\sigma N_s$

$$F_{RXN} = \frac{12.5\Delta\sigma^2}{\mu}$$

Rigid GB $N_s = \frac{3f_v}{2\pi r^2}$

Flexible GB $N_s = \frac{3f_v^{2/3}}{4\pi r^2}$

	F_{PIN}	F_{RXN}
High-Nb	0.0323MPa	0.525 MPa
Low-Nb	0.0141MPa	0.151 MPa

E.J. Palmiere, et al (1996)

Complex particles persist

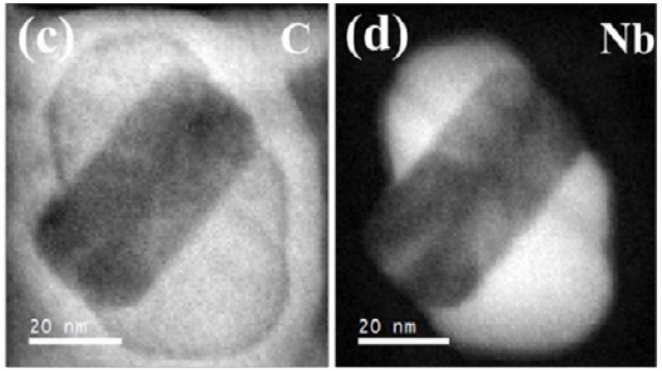

X. Ma, C. Miao, B. Langelier, S. Subramanian, Materials & Design 132 (2017) 244-249.

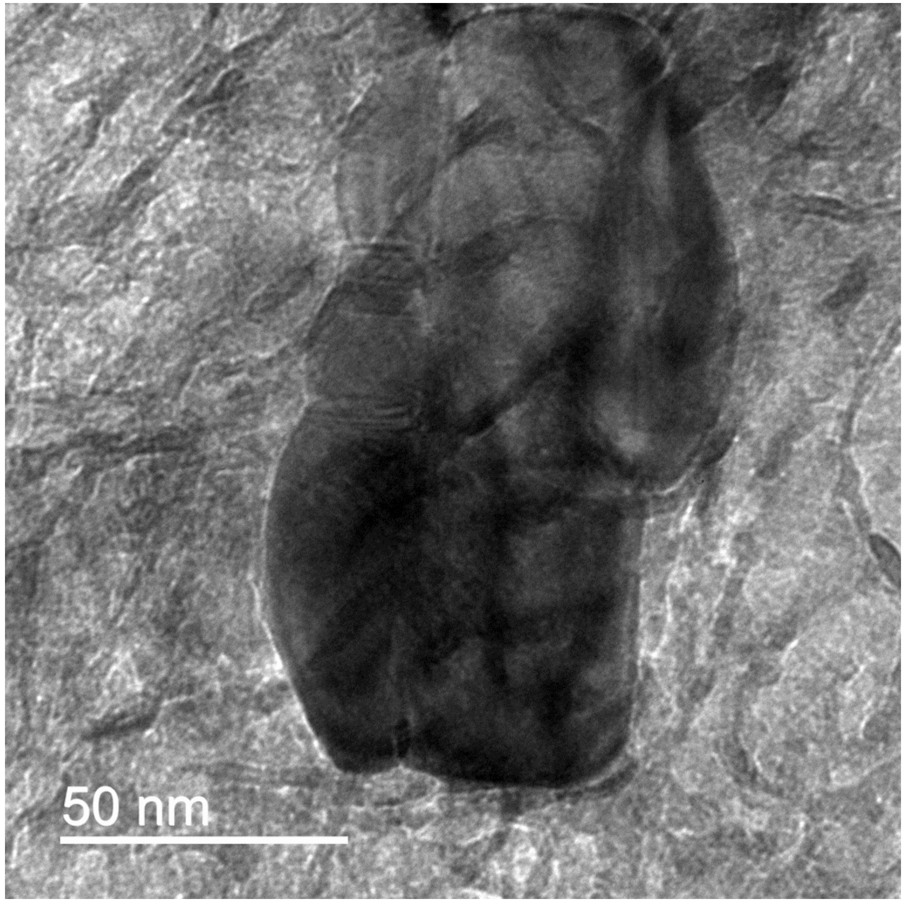

	At%
C	6.4
N	14.6
O	66.42
Si	0.13
S	
Cl	0.5
Ti	0.72
V	0.02
Cr	0.02
Mn	0.04
Fe	2.02
Ni	0
Cu	0.08
Nb	9.06

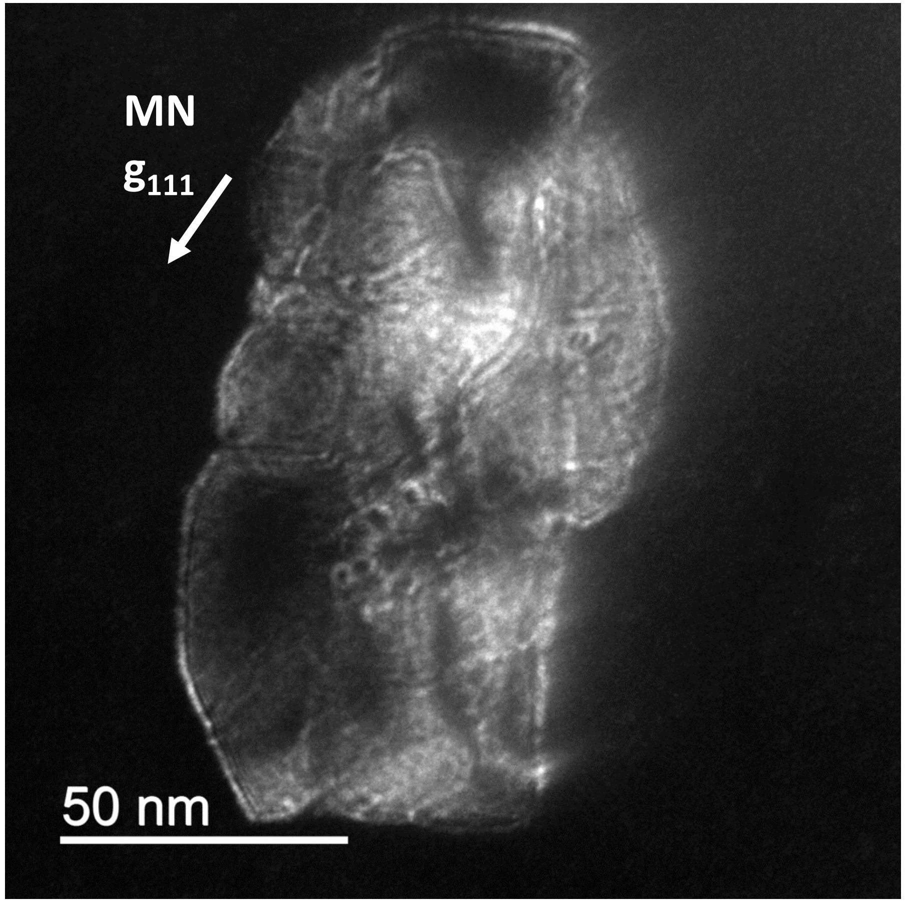

Experimental Approach - Results

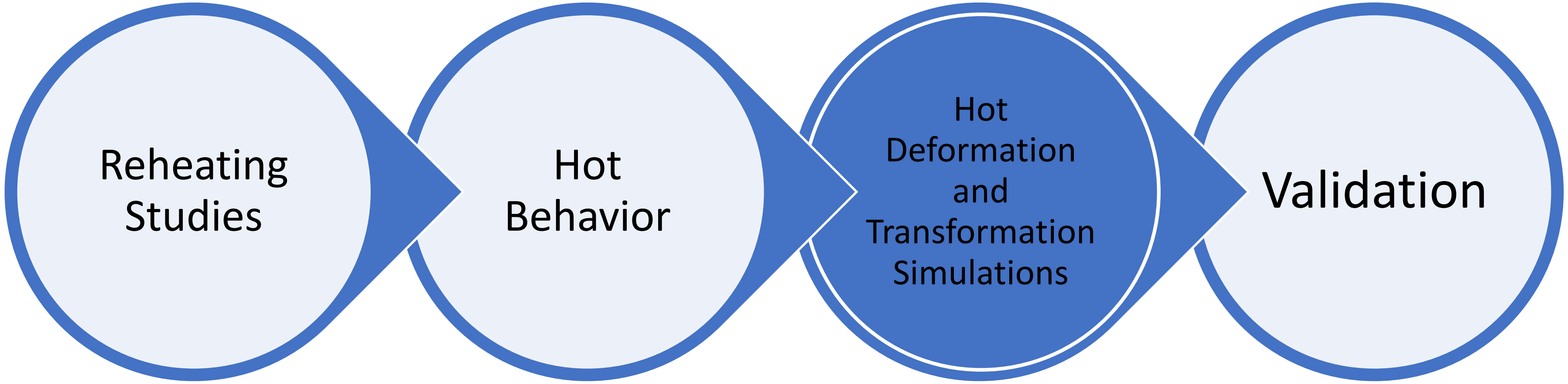

Reheating Studies

- Grain coarsening
- Dissolution study

Hot Behavior

- MFS
- Recrystallization
- Precipitation studies

Hot Deformation and Transformation Simulations

- Austenite conditioning
- Ferrite formation
- Precipitation

Validation

- Full scale validation at experimental mill

University of Pittsburgh

IRCR Offers More Nucleation Area After Roughing

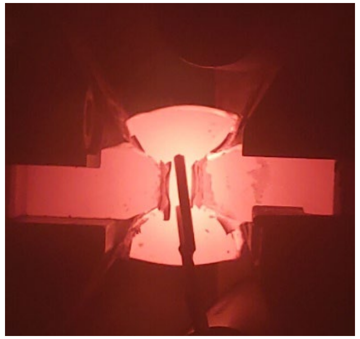

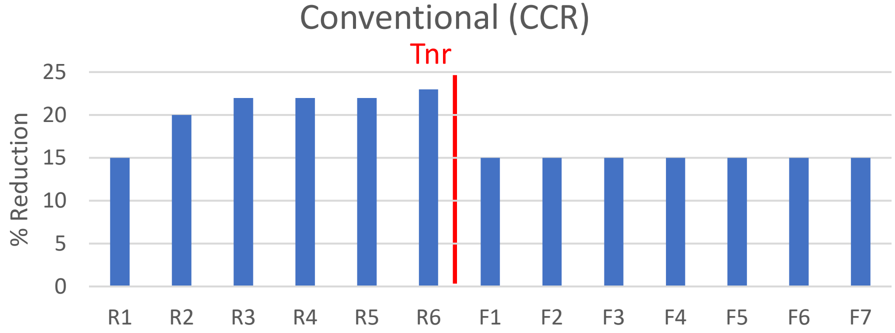

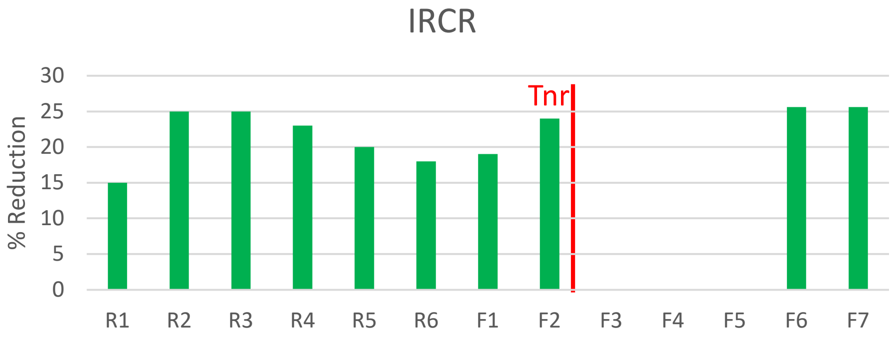

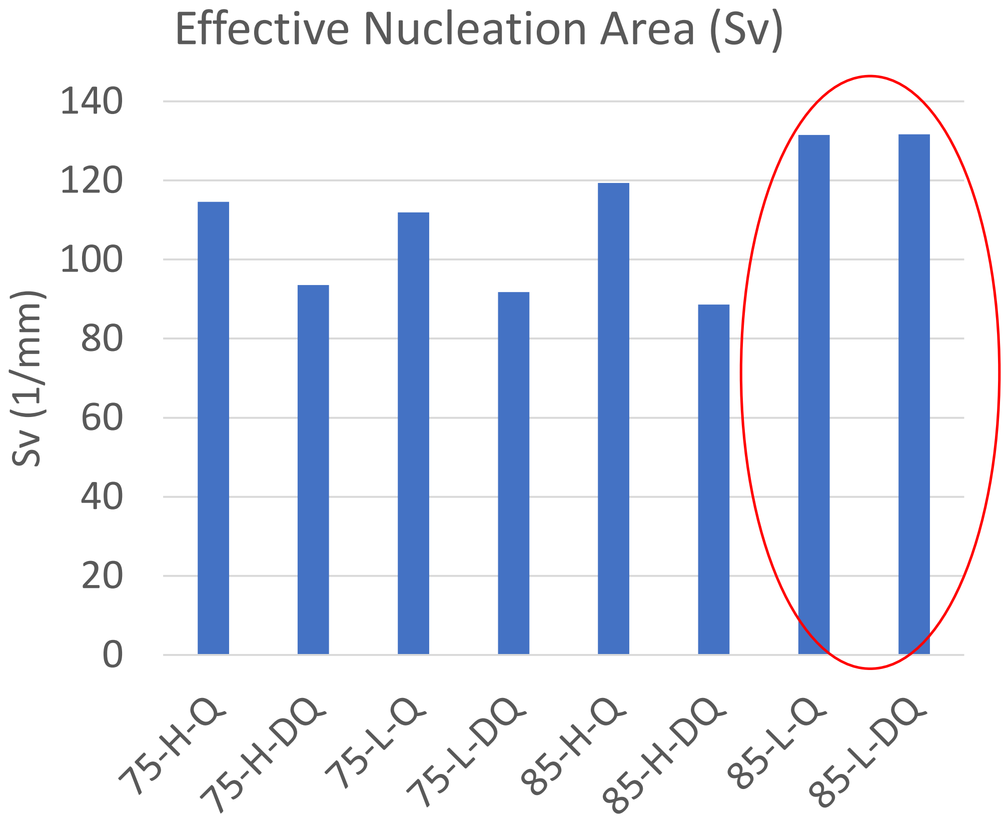

$$S_V(gb+db) = 0.429(N_L)_{||} + 1.571(N_L)_{\perp}$$

T. Kvackaj, I. Mamuzic(1998).

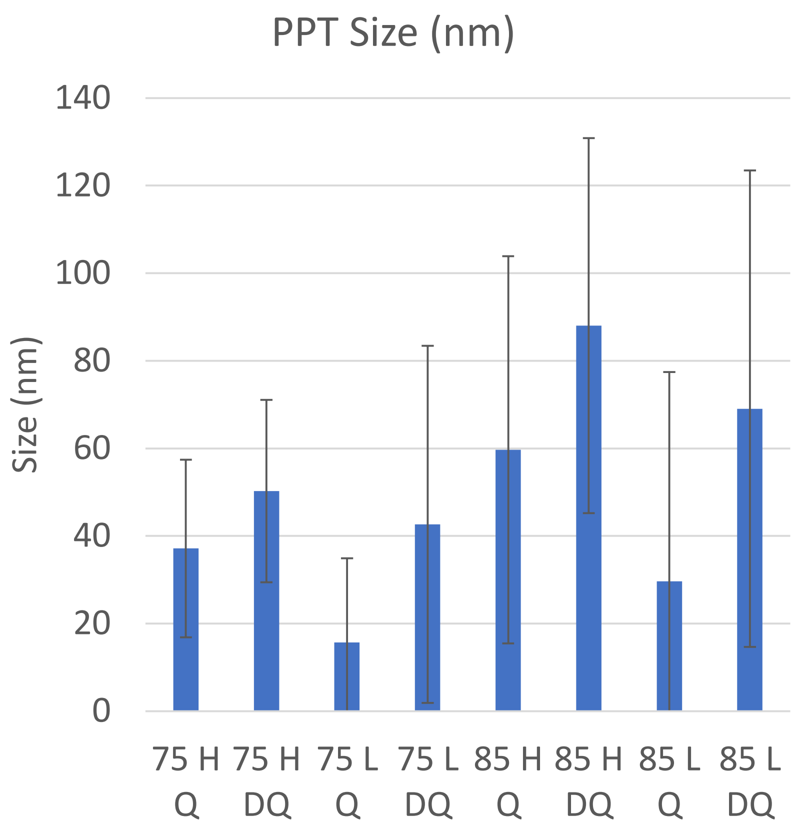
PPT Size (nm)
Size (nm)
140
120
100
80
60
40
20
0
75 H Q
75 H DQ
75 L Q
75 L DQ
85 H Q
85 H DQ
85 L Q
85 L DQ

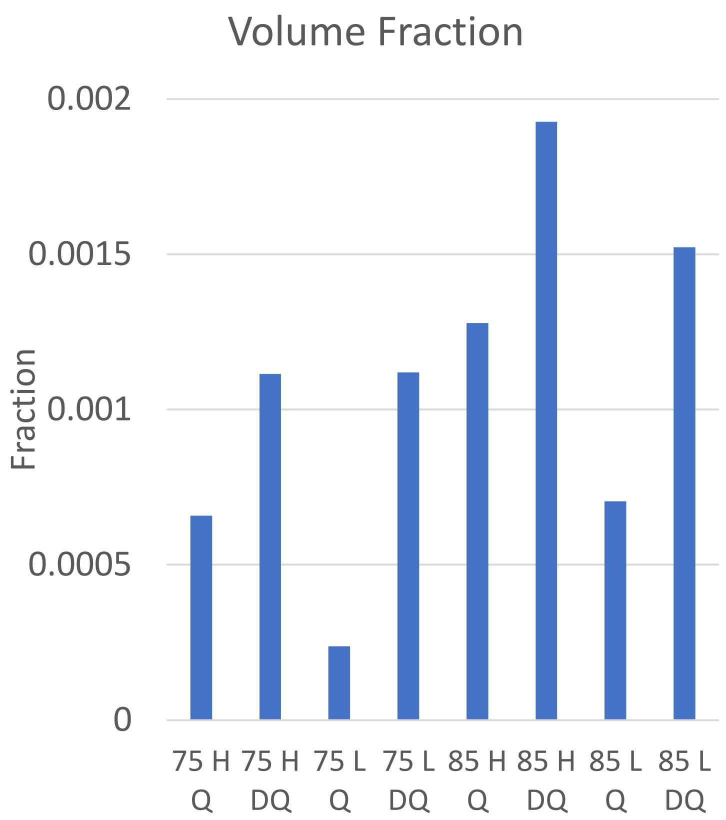
Volume Fraction
Fraction
0.002
0.0015
0.001
0.0005
0
75 H Q
75 H DQ
75 L Q
75 L DQ
85 H Q
85 H DQ
85 L Q
85 L DQ

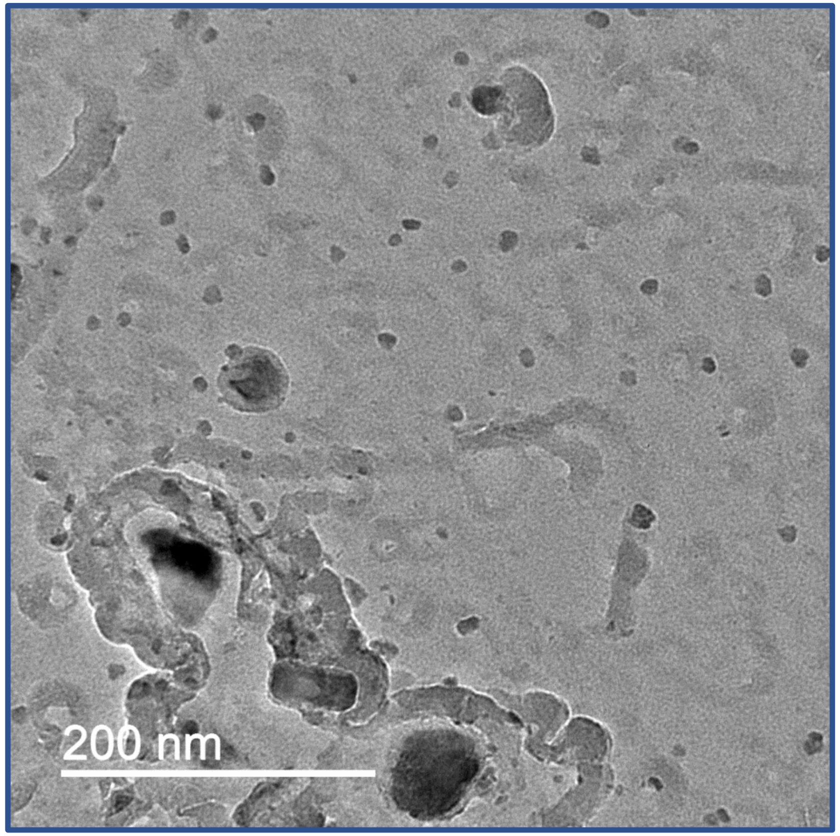
200 nm

IRCR High Nb – After Transfer

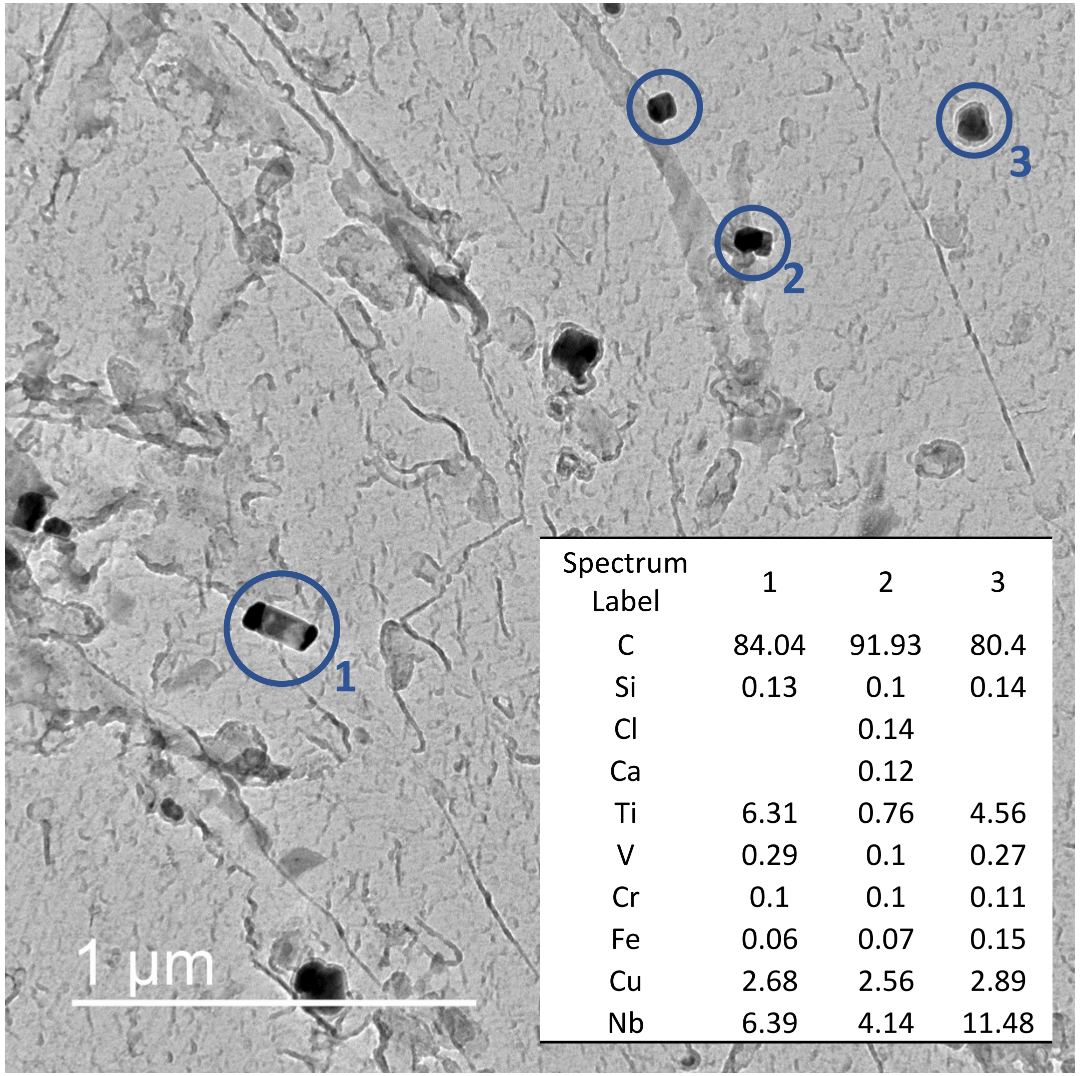

Spectrum Label	1	2	3
C	84.04	91.93	80.4
Si	0.13	0.1	0.14
Cl		0.14	
Ca		0.12	
Ti	6.31	0.76	4.56
V	0.29	0.1	0.27
Cr	0.1	0.1	0.11
Fe	0.06	0.07	0.15
Cu	2.68	2.56	2.89
Nb	6.39	4.14	11.48

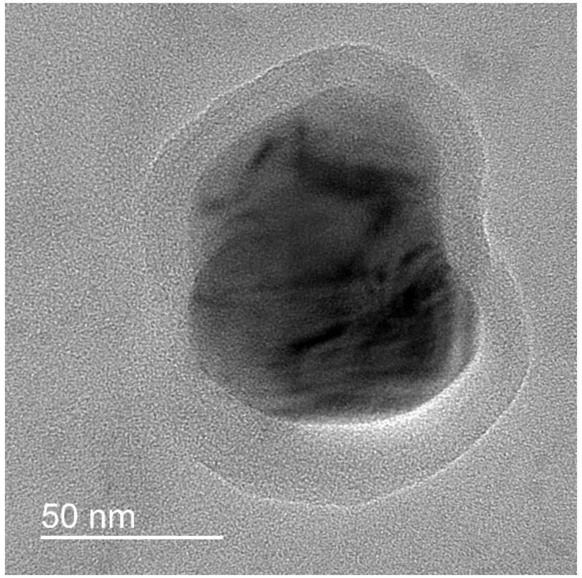

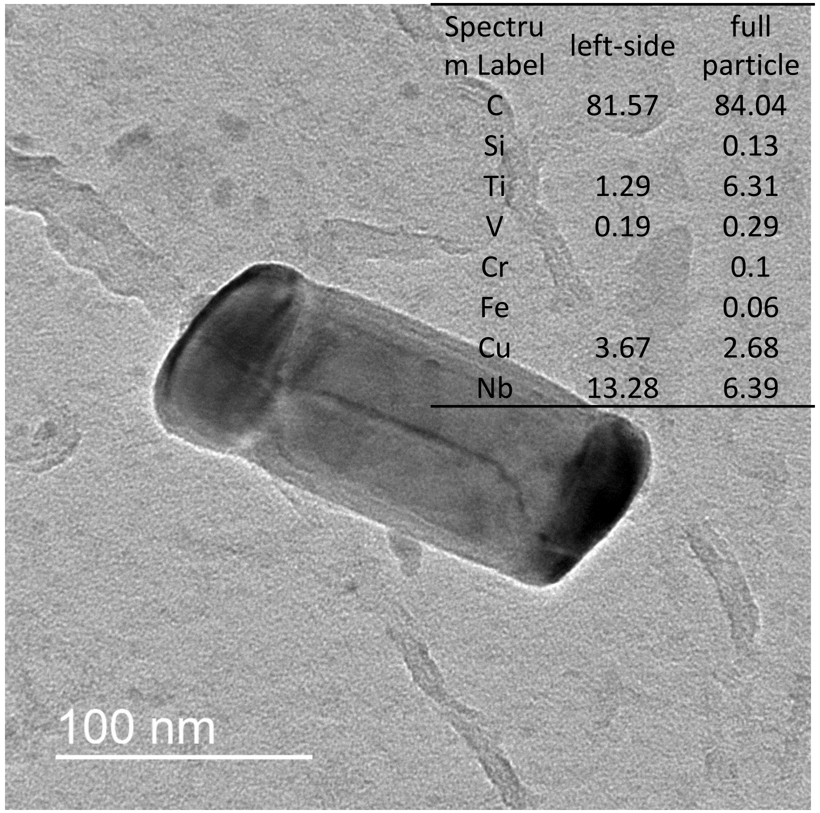

Spectrum Label	left-side	full particle
C	81.57	84.04
Si		0.13
Ti	1.29	6.31
V	0.19	0.29
Cr		0.1
Fe		0.06
Cu	3.67	2.68
Nb	13.28	6.39

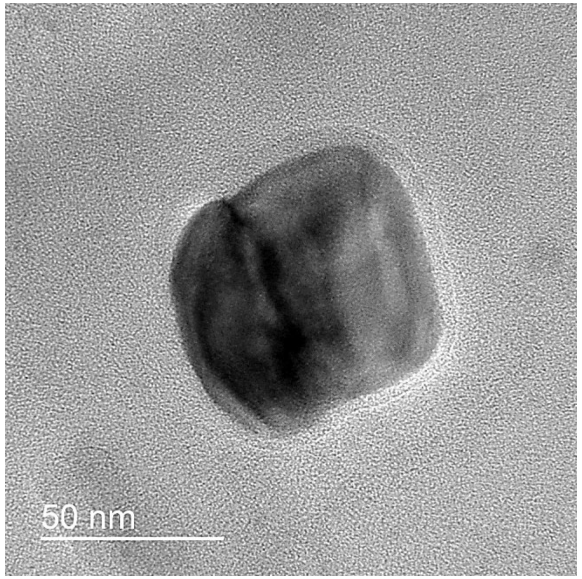

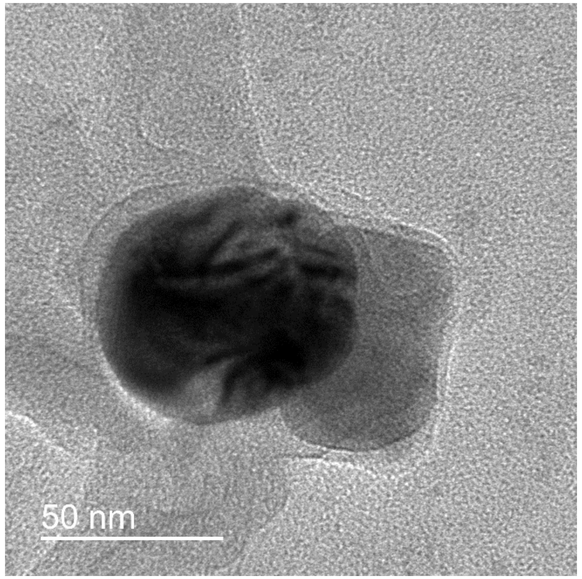

Precipitate Size Distribution (20 000X)

University of Pittsburgh

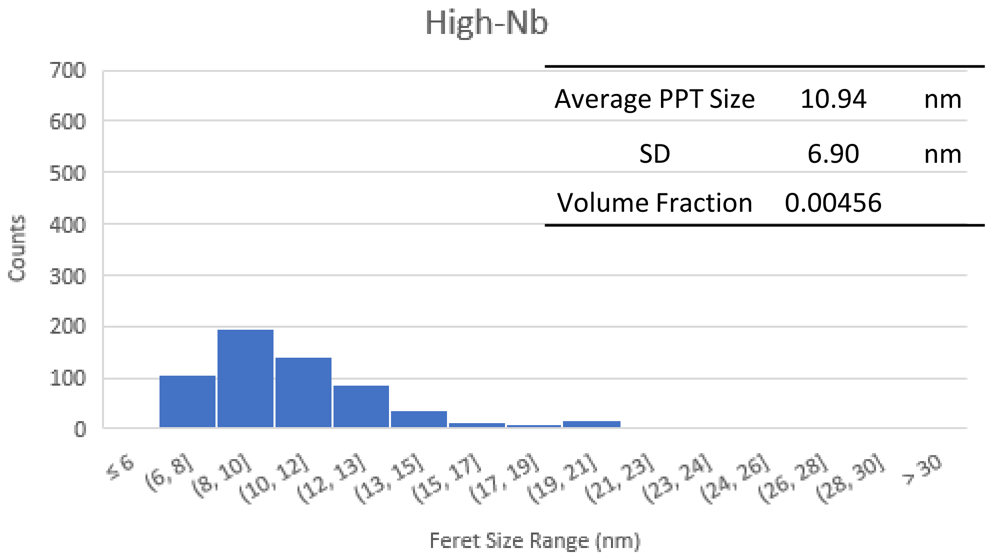

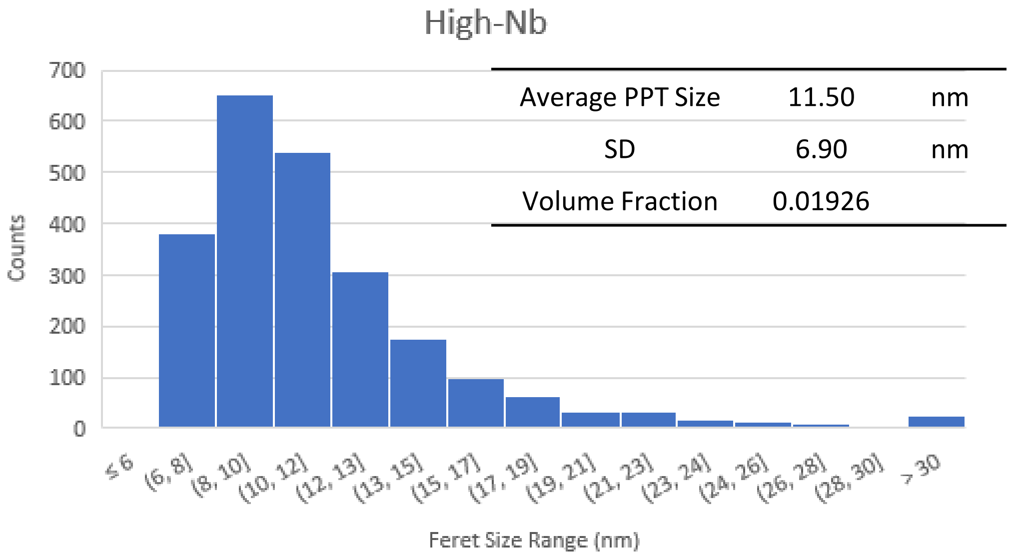

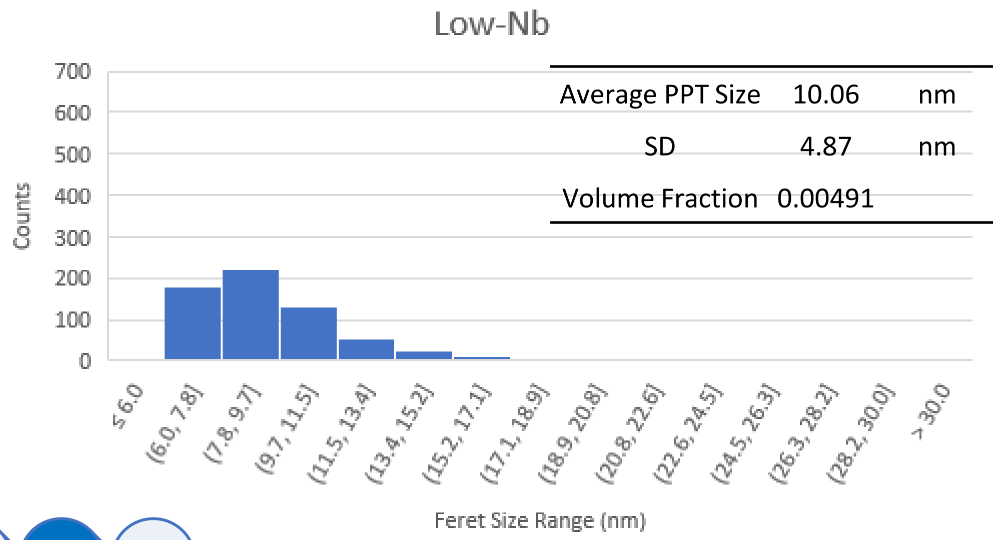

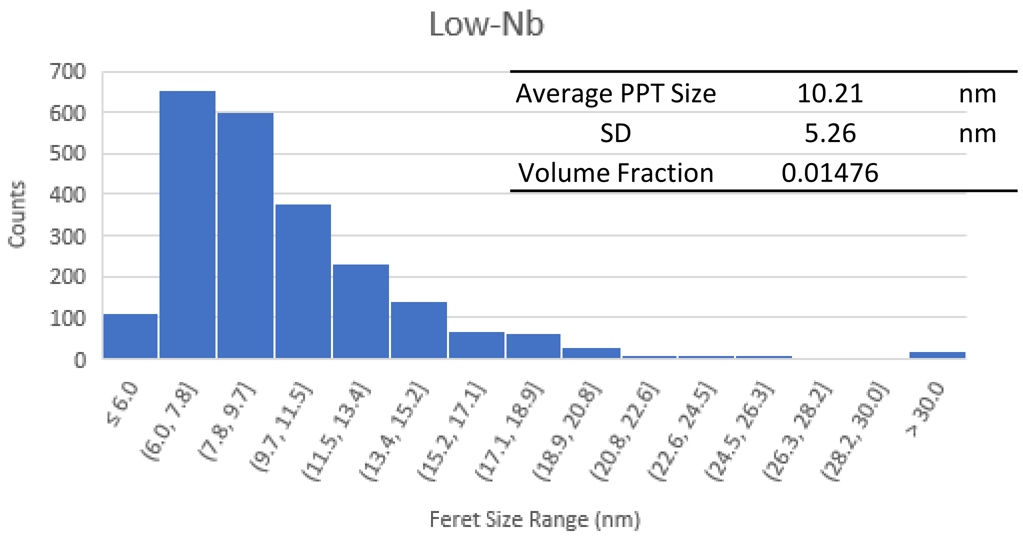

1 2 3 4

BEFORE TRANSFER

AFTER TRANSFER

Recrystallization vs Pinning Force

E.J. Palmiere, C.I. Garcia, A.J. DeArdo, Metallurgical and Materials Transactions A 27(4) (1996) 951-960.

Zener: $F_{PIN} = 4r\sigma N_s$

$$F_{RXN} = \frac{12.5\Delta\sigma^2}{\mu}$$

Flexible GB

$$N_s = \frac{3f_v^{2/3}}{4\pi r^2}$$

	PPT Average Feret Diameter (nm)	Volume Fraction	F_{PIN} (MPa)	F_{RXN} (MPa)
High-Nb Roughing	10.94	0.00456	3.84	0.1075
High-Nb Transfer	11.50	0.01926	9.55	0.1075
Low-Nb Roughing	10.06	0.00491	4.39	0.1744
Low-Nb Transfer	10.21	0.01476	8.94	0.1744

Simulation of Finishing

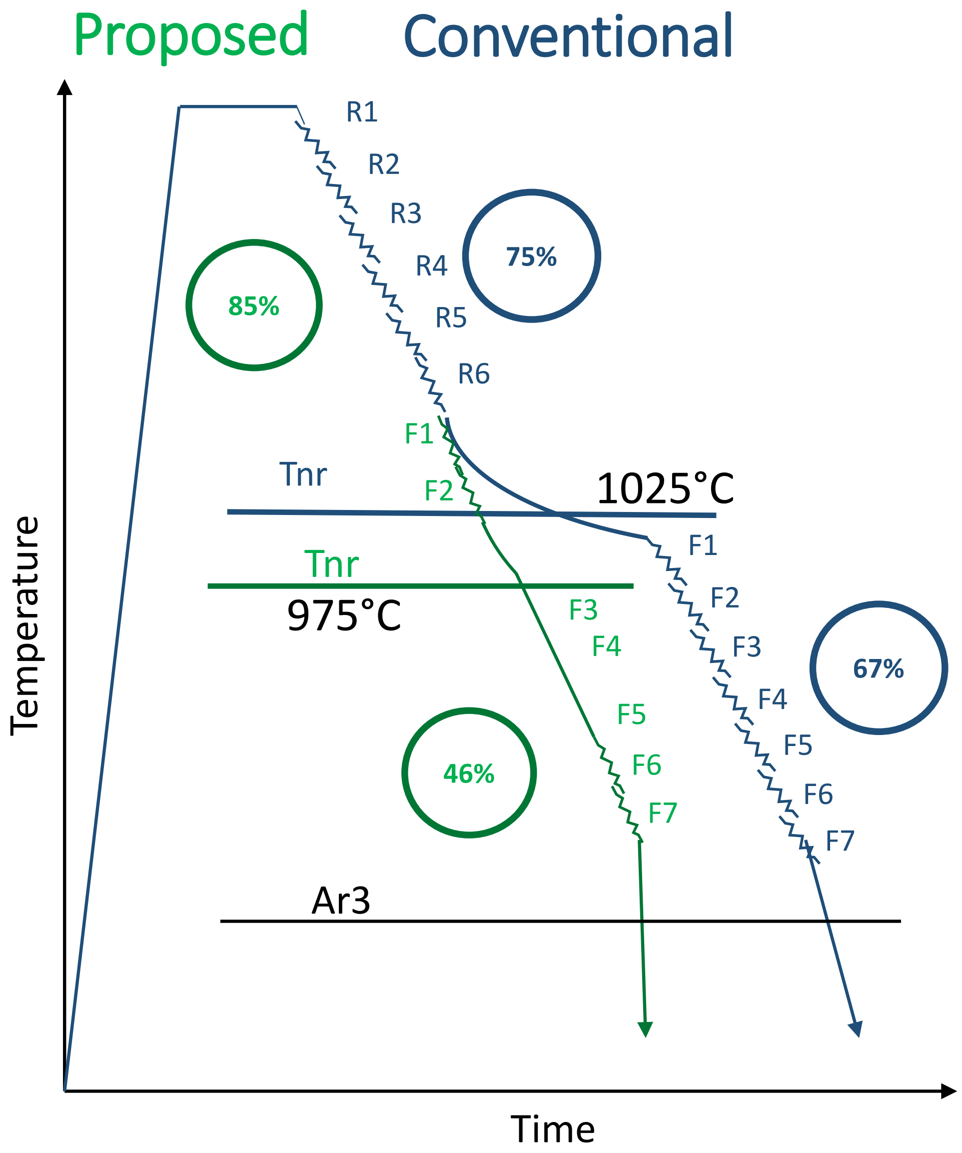

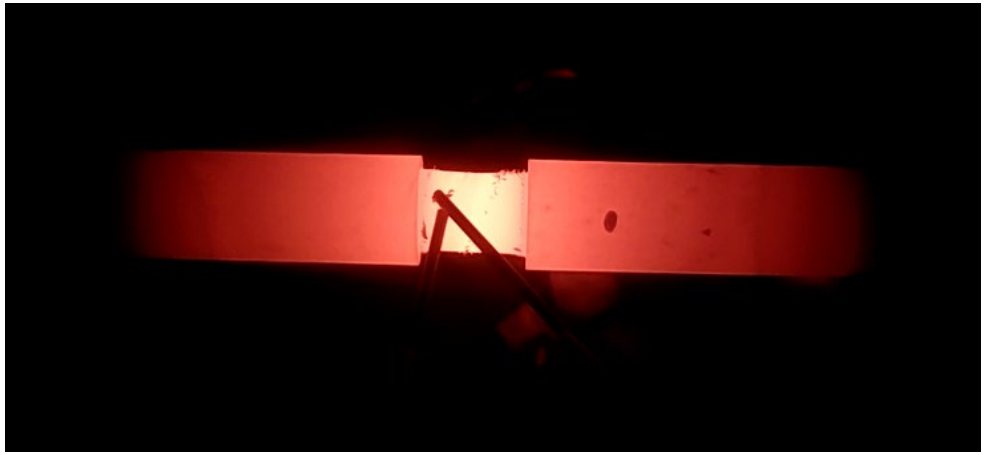

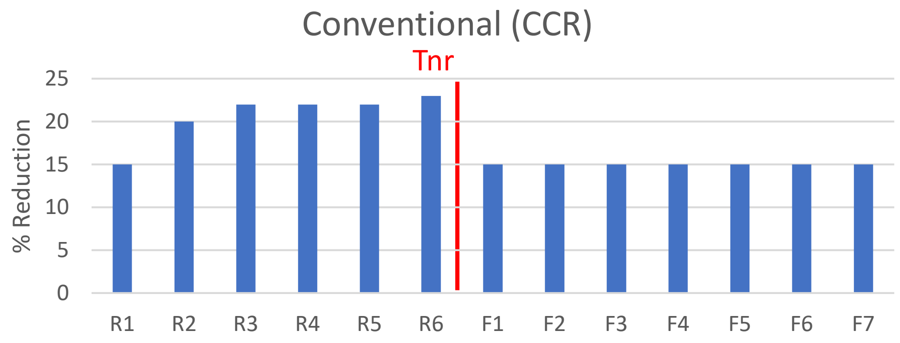

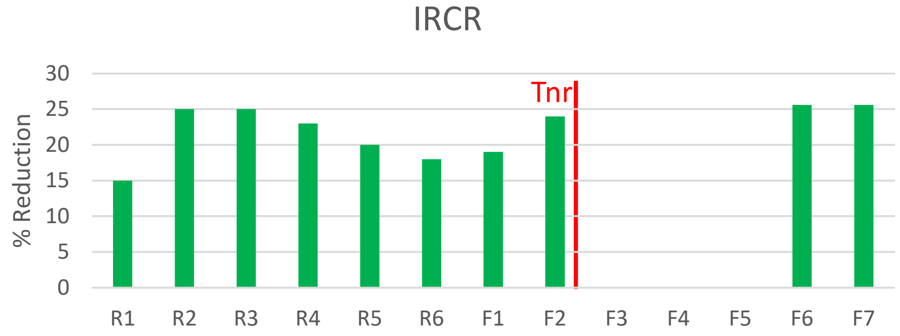

Summary: Hot Deformation

After Roughing:

- Precipitation is copious and $F_{PIN} > F_{RXN}$
- Average austenite grain size is similar for both process
- Effective nucleation area (Sv) is higher in IRCR

After Finishing:

- KAM is higher in IRCR process
- Austenite conditioning promised numerous nucleation sites.

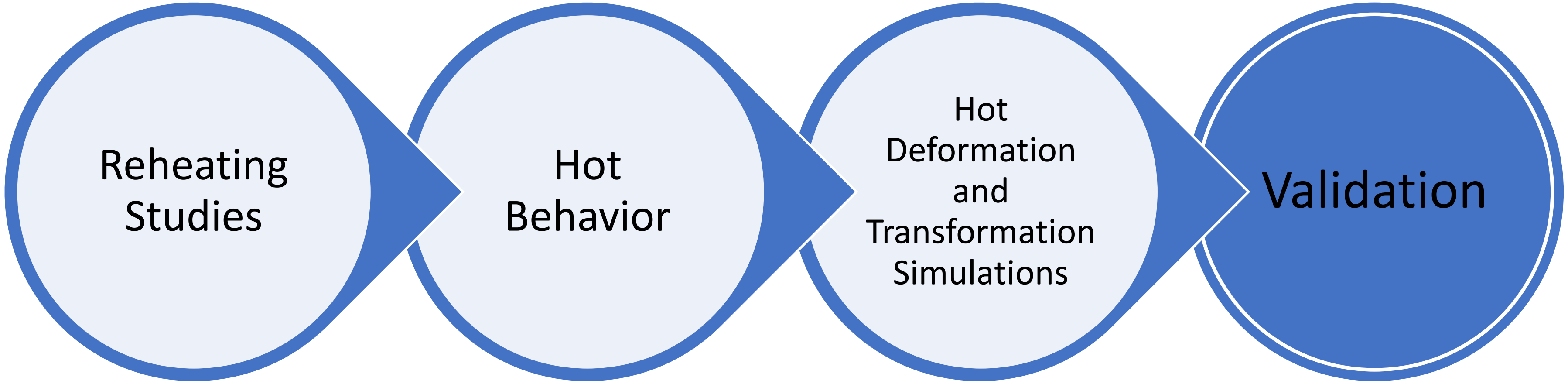

- Grain coarsening
- Dissolution study

- MFS
- Recrystallization
- Precipitation studies

- Austenite conditioning
- Ferrite formation
- Precipitation

- Full scale validation at experimental mill

University of Pittsburgh

Rolling Schedules

CCR

Tin (°C)	% Reduction	
1200		
1050	35.7	T>Tnr
925	24	T<Tnr Total Reduction 67%
900	24	
875	24	
850	24	
550		

IRCR

Tin (°C)	% Reduction	
1200		
1100	18	T>Tnr Total Reduction 61%
1070	27	
1040	35	
910	26	T<Tnr Total Reduction 45%
880	26	
550		

Accelerated Cooling of 16°C/s Was Used

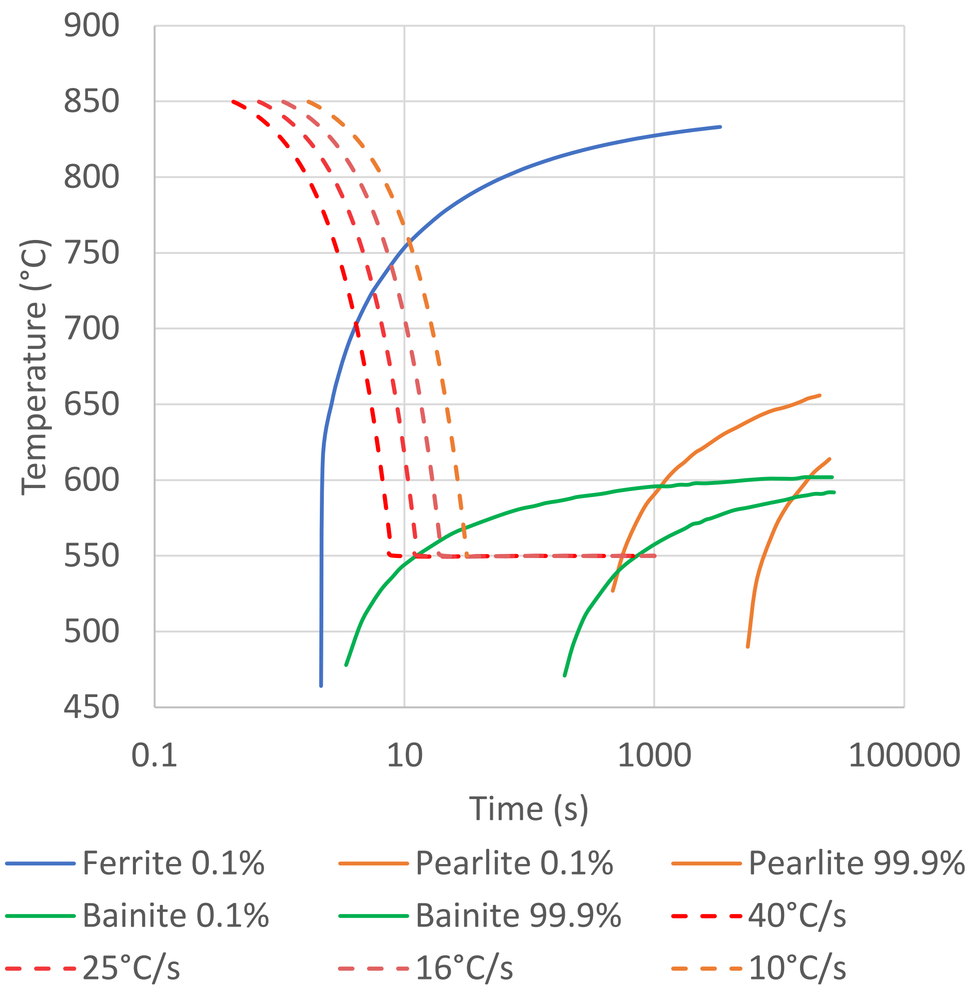

Observations	Source
0.09 and 0.04 Nb, 0.06 C, 2 Mn Optimum performance: 820°C finish, 460°C coiling, **25°C/s** cooling rate. API X100 achieved	L. Lan, et al (2017)
0.025 C, 0.04 Nb, 1.5 Mn, 0.32 Mo To obtain AF, **20°C/s** down to 400°C, followed by 1hr at 500°C. API X70 achieved.	M.-C. Zhao, et al (2003)
AF forms at temperature slightly above Bainitic transformation. NbC PPTN hardening in AF has high potency at 600°C holding.	Y. Gu, et al (2016)
0.14 C, 0.02 Nb, 0.96 Mn, 0.32 Mo **3°C/s** cooling rate enough to produce F-AF microstructure. Heterogeneous microstructure, undeformed austenitization.	L. Shi, et al (2014)
0.05 C, 0.1 Nb+V+Ti, 1.24 Mn 9-10°C/s form PF-AF microstructure after hot deformation in austenite. 10-12 and 14-17°C/s give more homogeneous structure, but USE and FATT similar to 9-10°C/s.	B. Hwang, et al (2005)

1 2 3 4

University of Pittsburgh

CCR High-Nb ACC

Boundaries: Rotation Angle

	Min	Max	Fraction	Number	Length
——	15°	65°	0.572	61786	5.35 mm

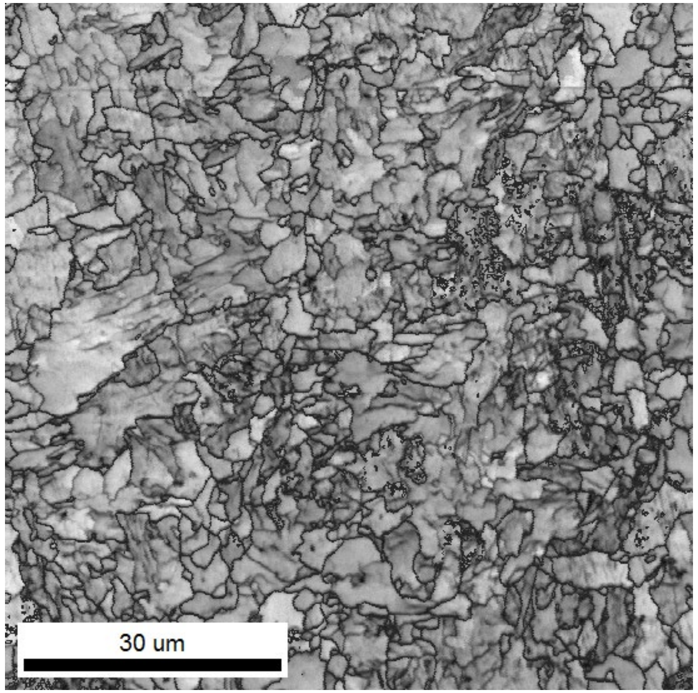

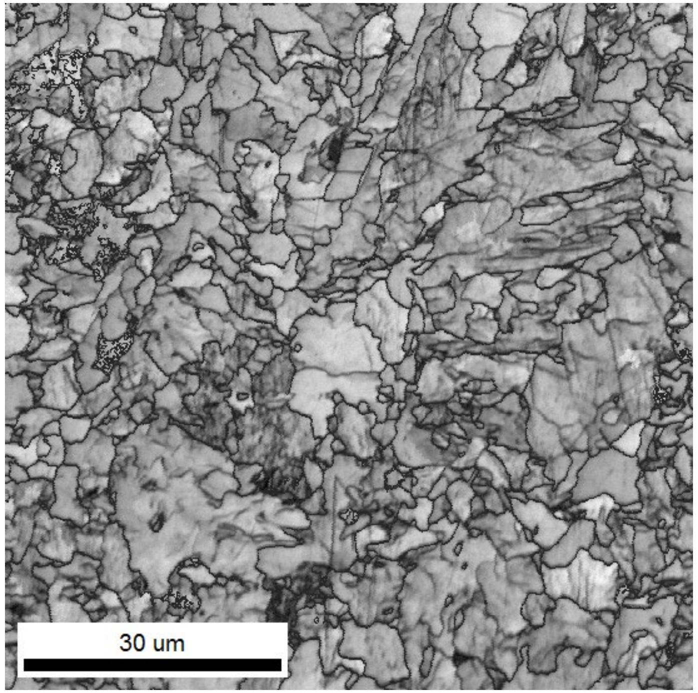

CCR Low-Nb ACC

Boundaries: Rotation Angle

	Min	Max	Fraction	Number	Length
——	15°	65°	0.602	53944	4.67 mm

IRCR High-Nb ACC

Boundaries: Rotation Angle

	Min	Max	Fraction	Number	Length
——	15°	65°	0.608	64111	5.74 mm

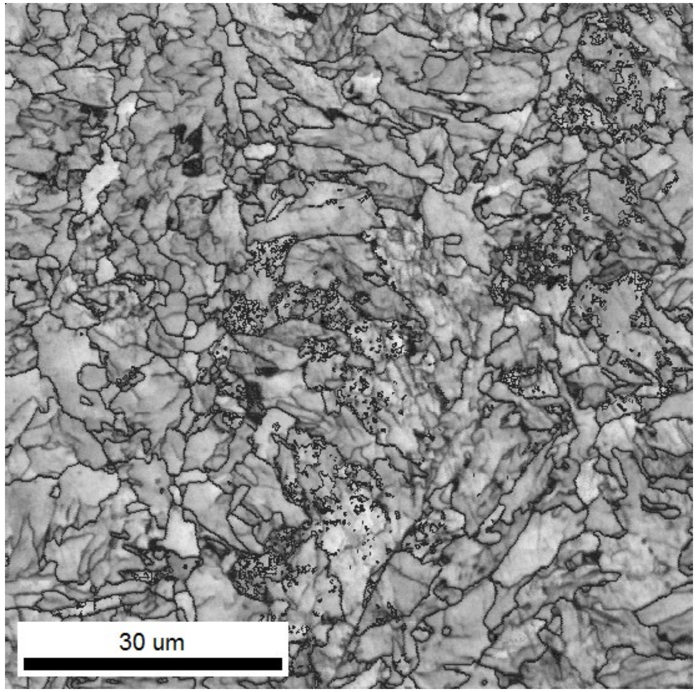

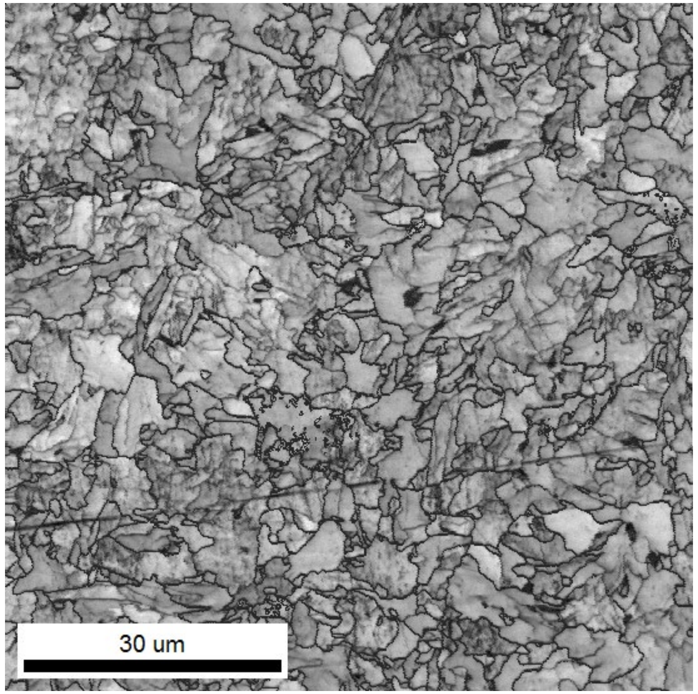

IRCR Low-Nb ACC

Boundaries: Rotation Angle

	Min	Max	Fraction	Number	Length
——	15°	65°	0.531	53629	4.64 mm

1 2 3 4

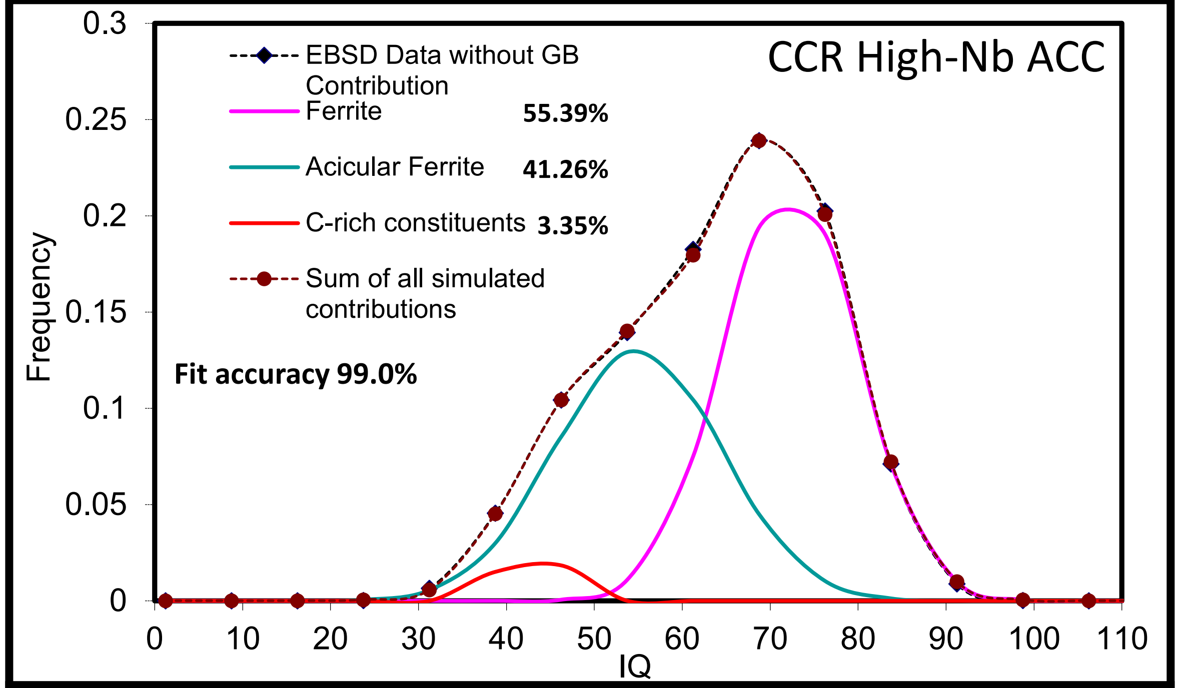
CCR High-Nb ACC
EBSD Data without GB Contribution
Ferrite 55.39%
Acicular Ferrite 41.26%
C-rich constituents 3.35%
Sum of all simulated contributions
Fit accuracy 99.0%
Frequency
IQ

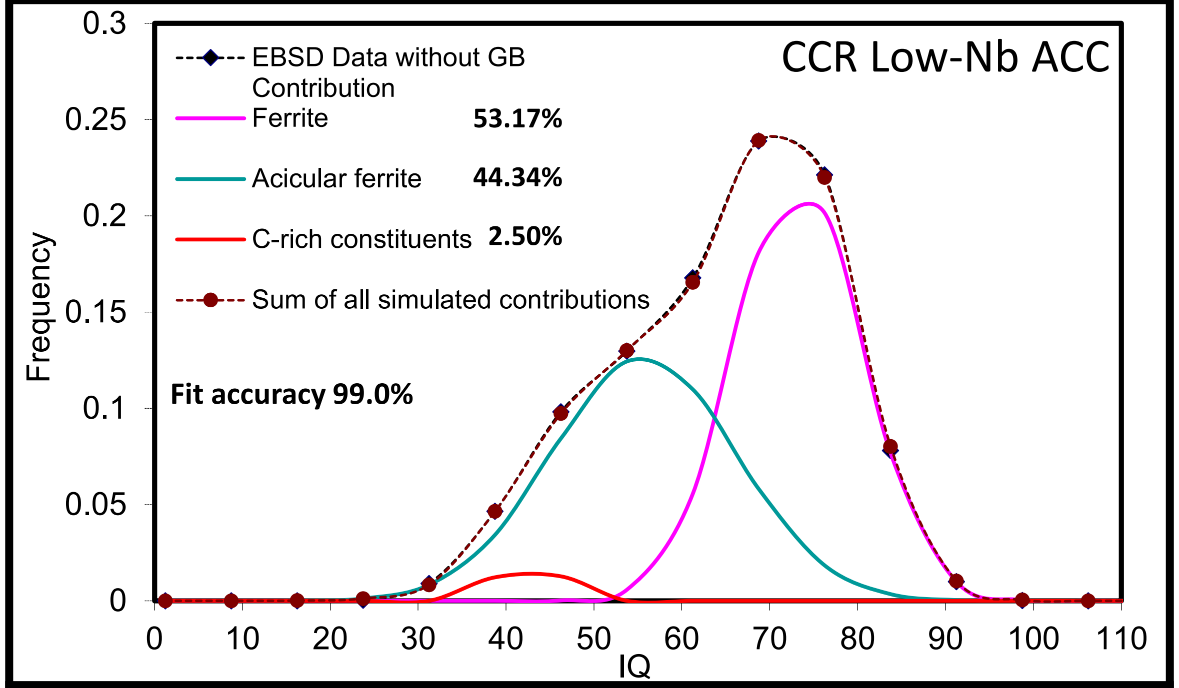
CCR Low-Nb ACC
EBSD Data without GB Contribution
Ferrite 53.17%
Acicular ferrite 44.34%
C-rich constituents 2.50%
Sum of all simulated contributions
Fit accuracy 99.0%
Frequency
IQ

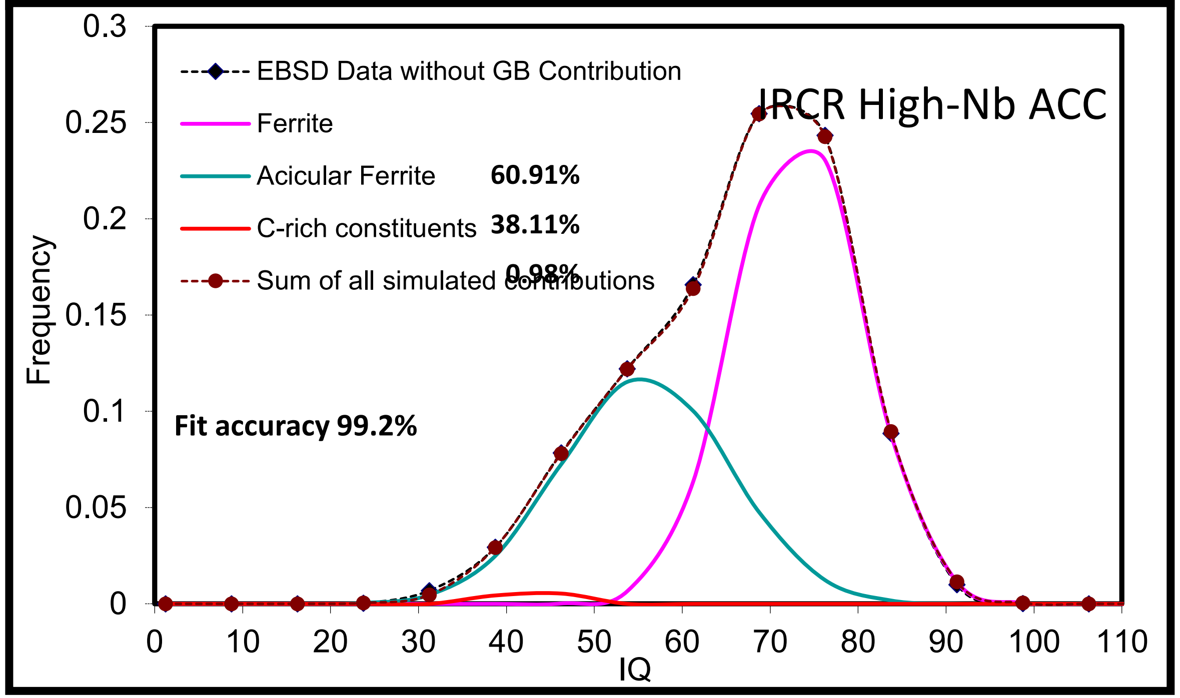
IRCR High-Nb ACC
EBSD Data without GB Contribution
Ferrite
Acicular Ferrite 60.91%
C-rich constituents 38.11%
Sum of all simulated contributions 0.98%
Fit accuracy 99.2%
Frequency
IQ

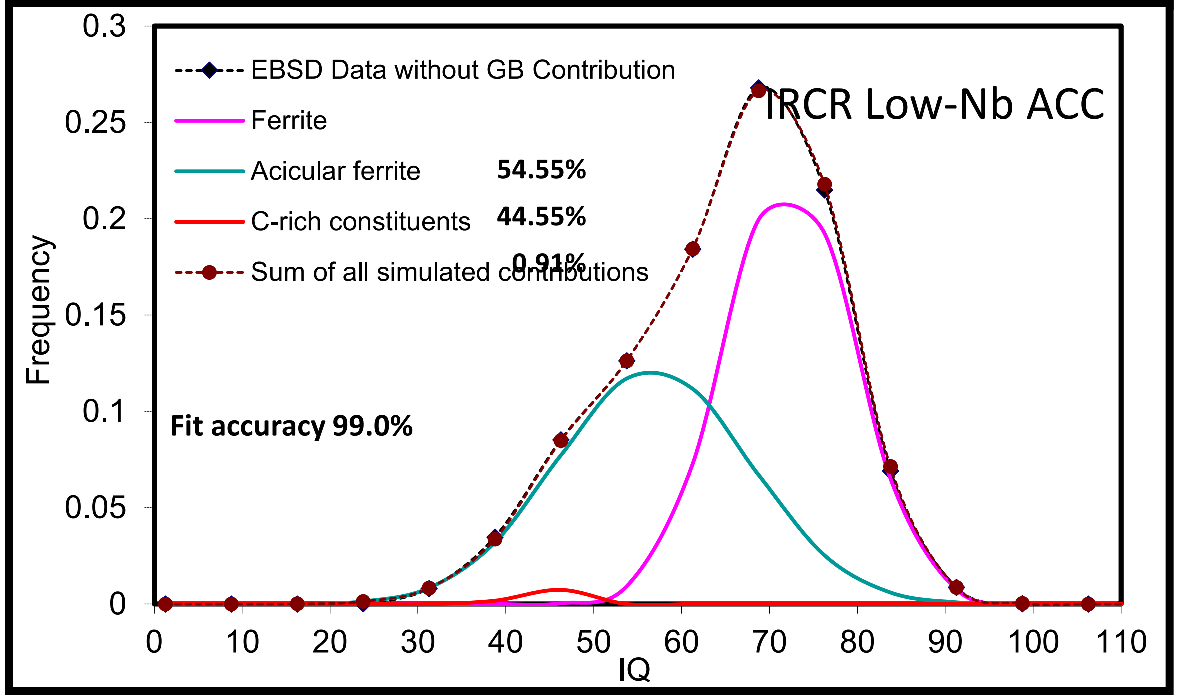
IRCR Low-Nb ACC
EBSD Data without GB Contribution
Ferrite
Acicular ferrite 54.55%
C-rich constituents 44.55%
Sum of all simulated contributions 0.91%
Fit accuracy 99.0%
Frequency
IQ

Higher UTS after IRCR

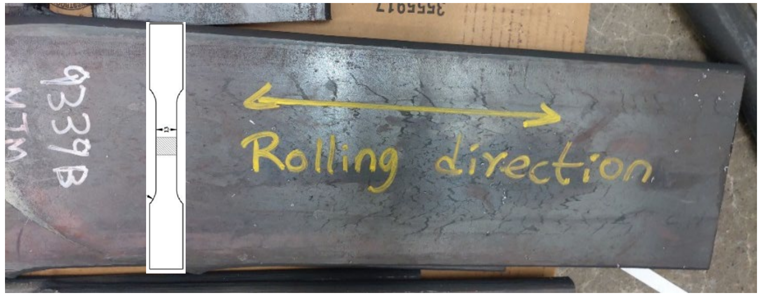

	YS (KSI)	UTS (KSI)	Elongation %
CCR High-Nb	78.73	93344	37.2%
CCR Low-Nb	75.25	89718	35.2%
IRCR High-Nb	70.54	95675	31.5%
IRCR Low-Nb	75.23	93336	31.4%

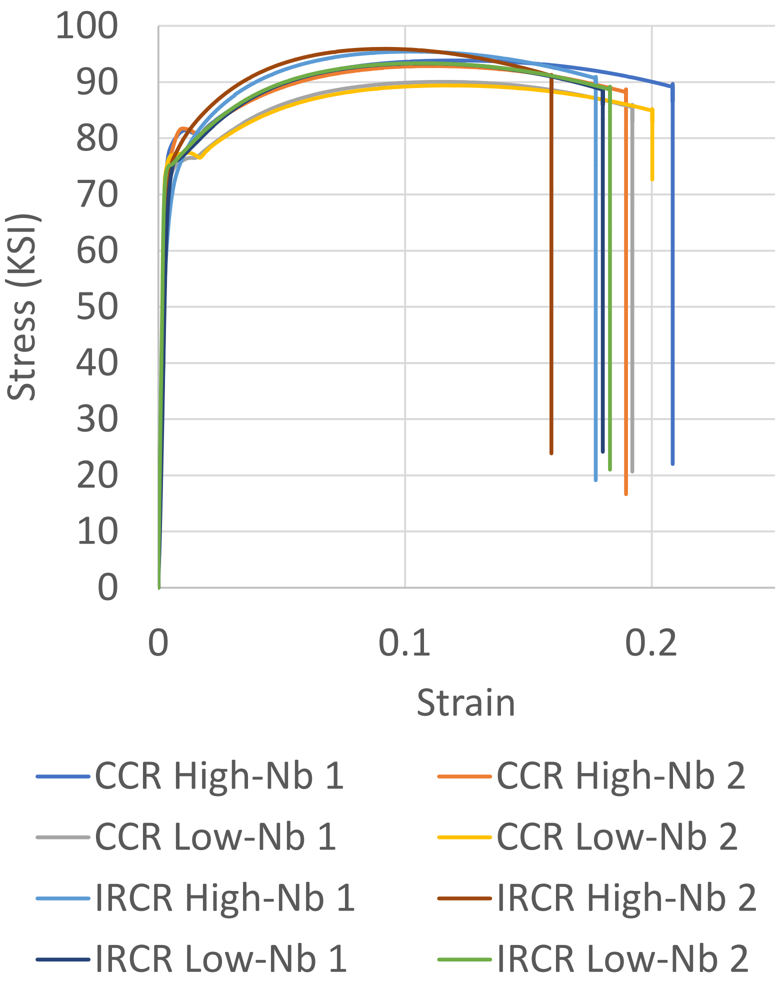

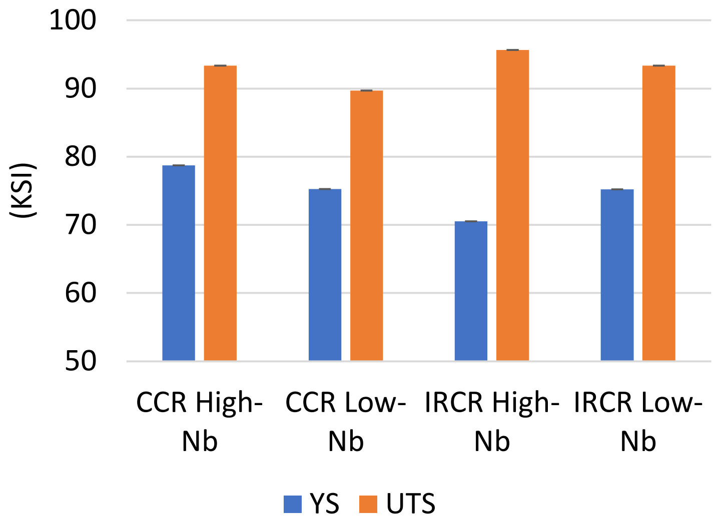

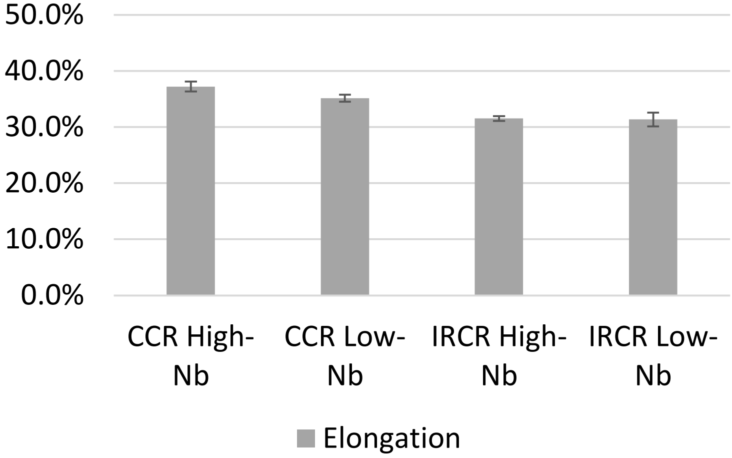

1 2 3 4

Splitting in CCR: Inhomogeneous microstructure

CCR High-Nb CCR Low-Nb IRCR High-Nb IRCR Low-Nb

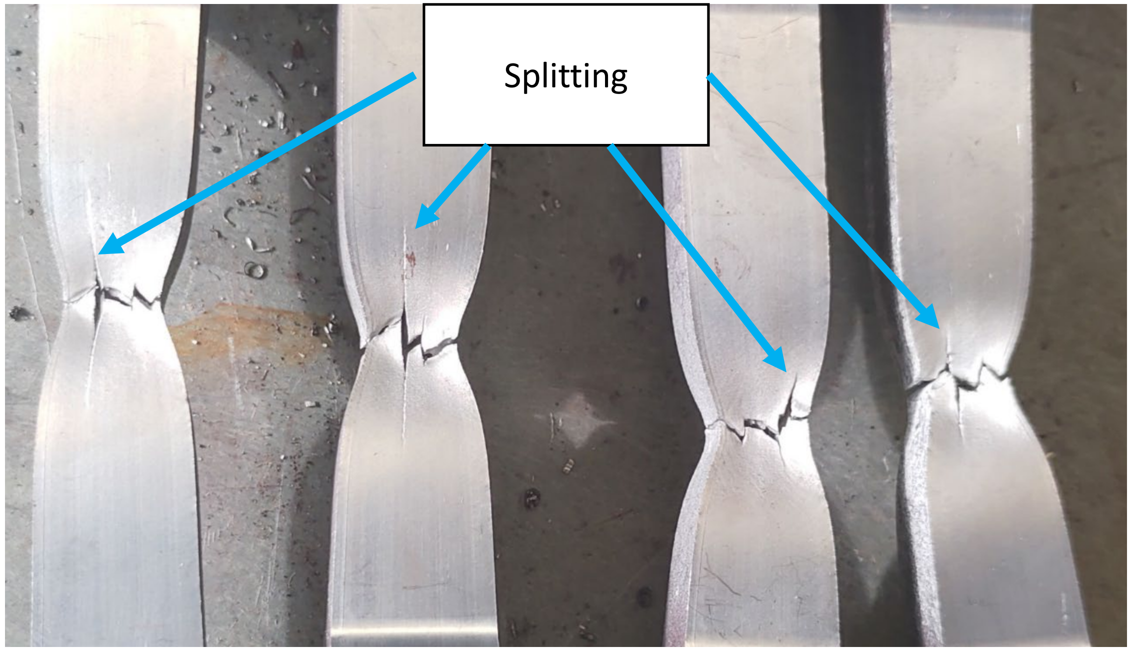

CVN: Low-Nb Tougher

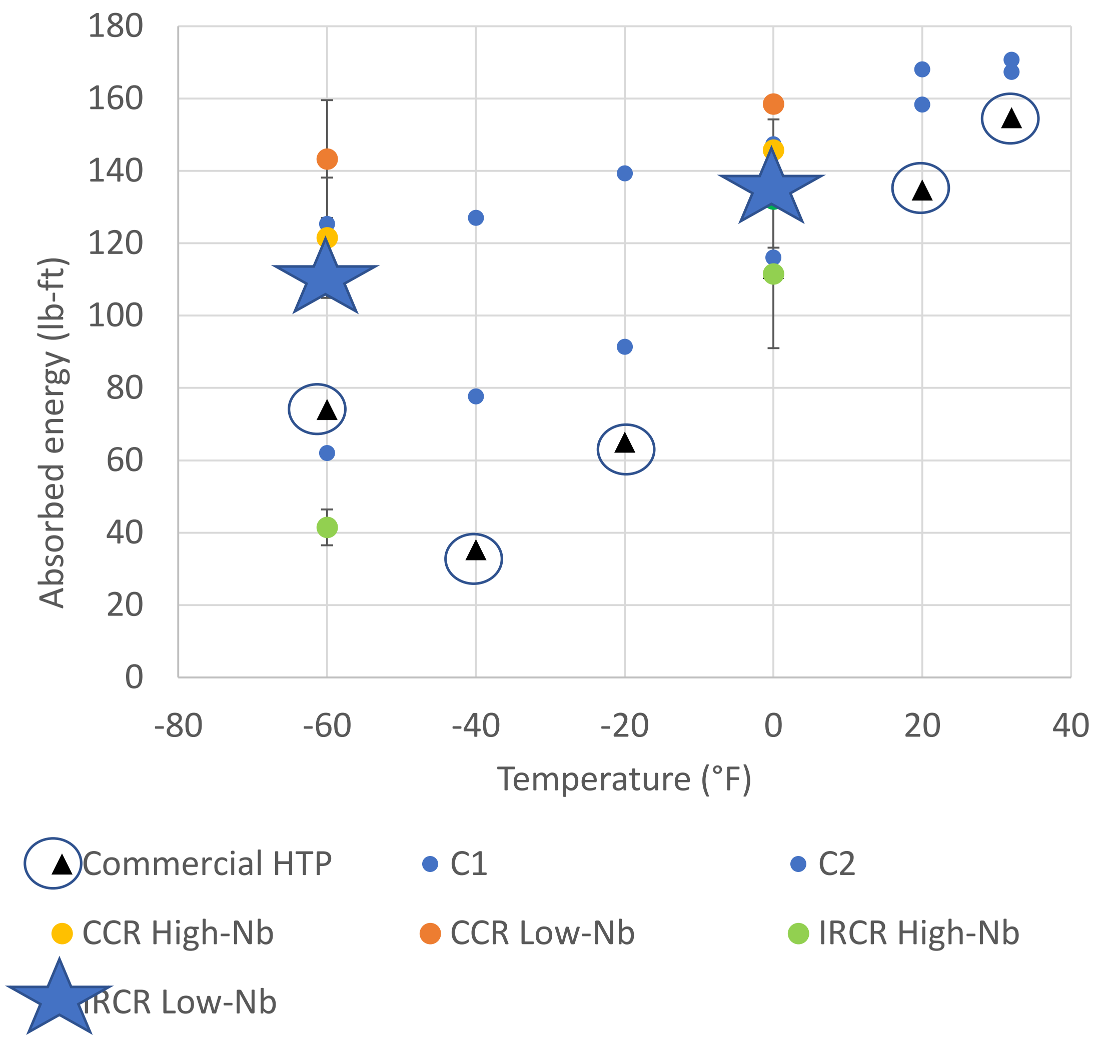

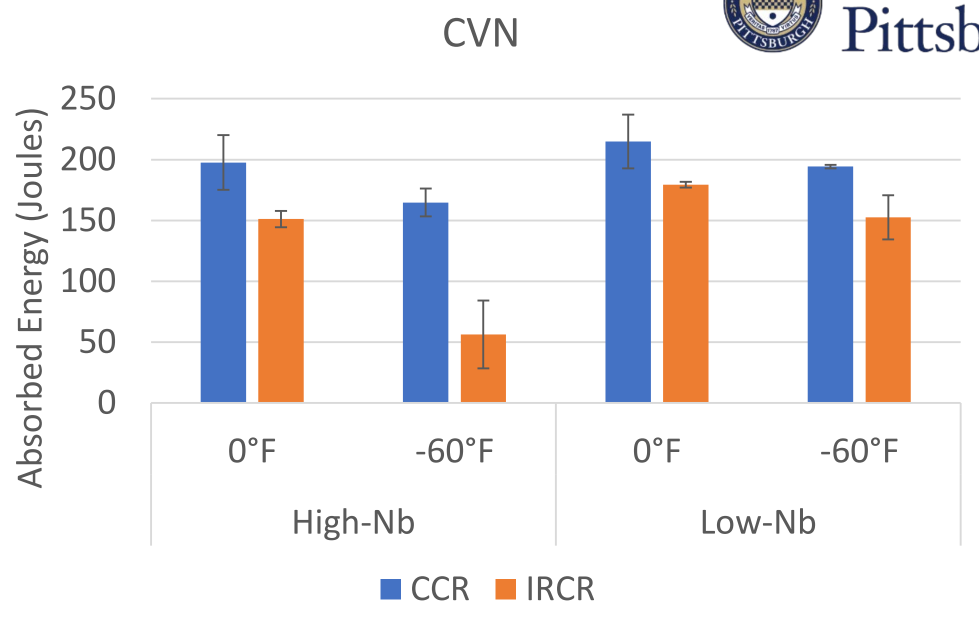

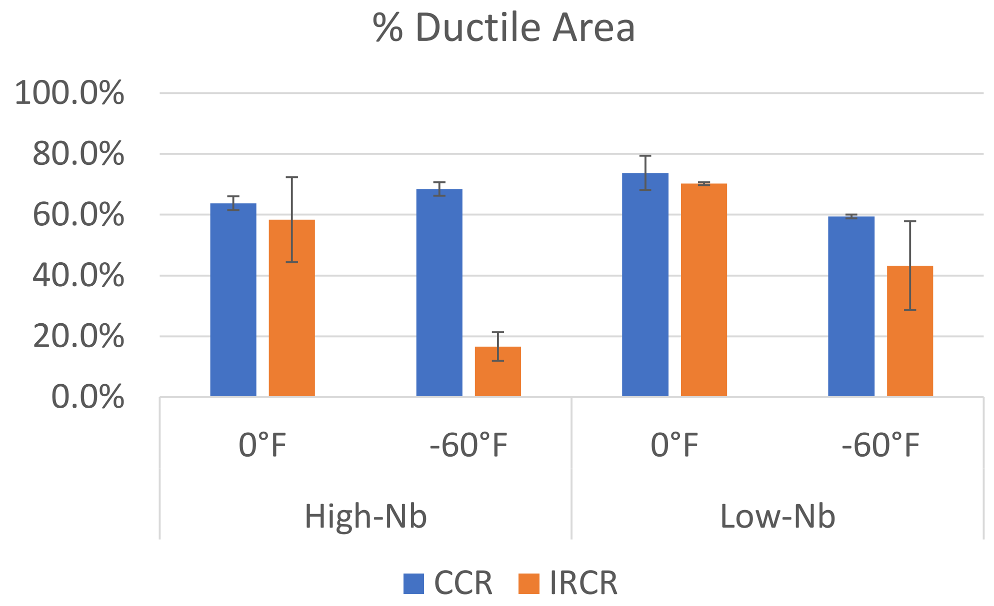

1 2 3 4

IRCR: Finer, More Homogeneous Grain Size

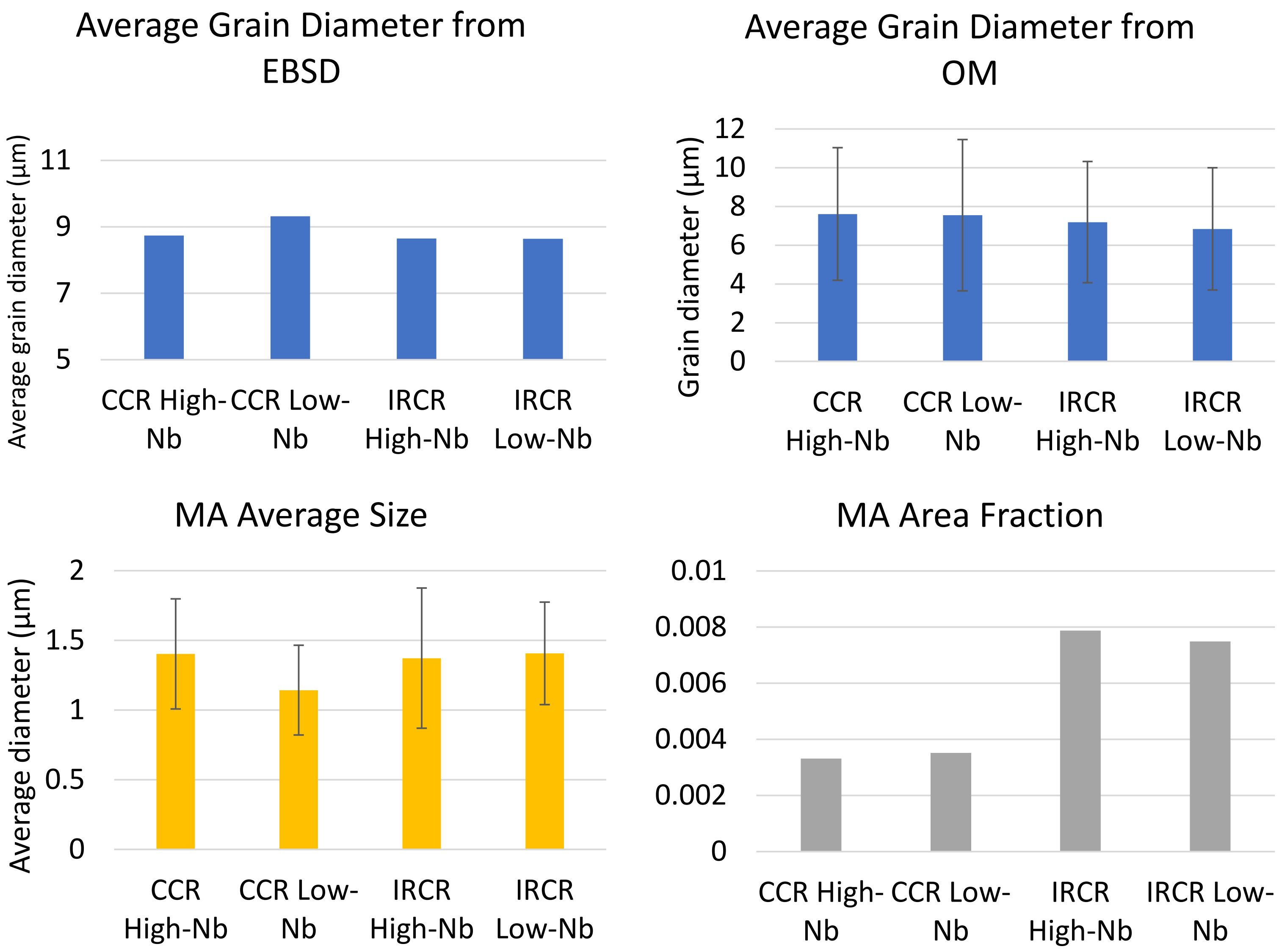

1 2 3 4

Final Precipitation is Finer in IRCR

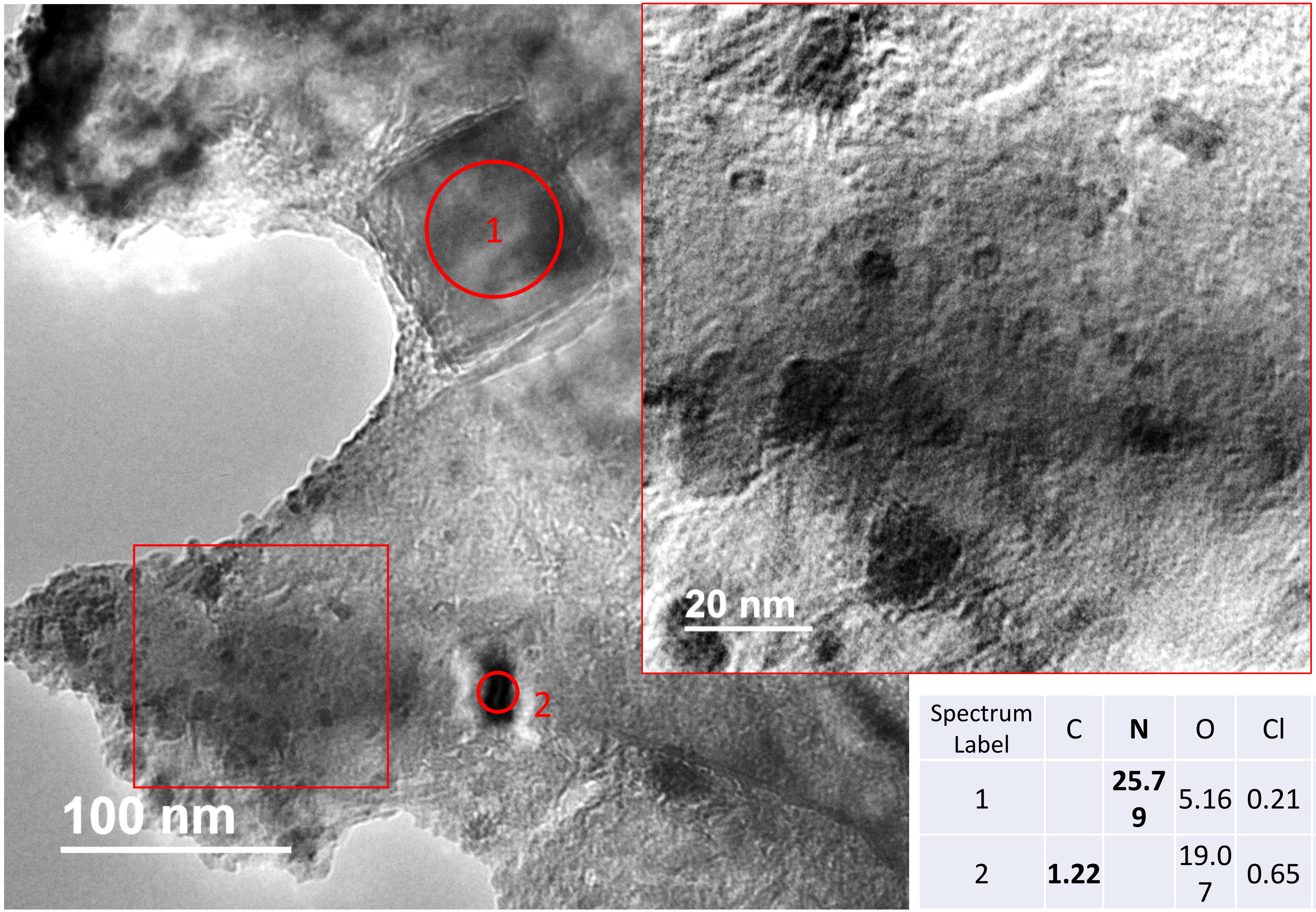

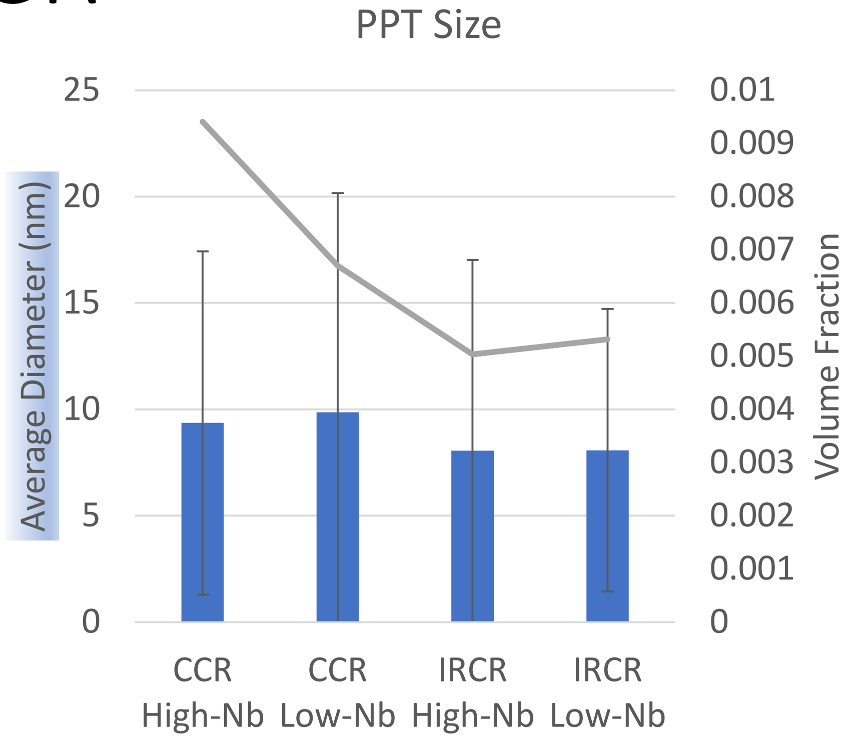

Spectrum Label	C	**N**	O	Cl	**Ti**	V	Mn	Fe	Cu	**Nb**	Mo
1		**25.79**	5.16	0.21	**29.32**	1.7	0.43	18.3	3.04	**16.06**	
2	**1.22**		19.07	0.65			0.9	68.07	8.07		**2.01**

Thank You!

University of Pittsburgh